



Supporting Information

Luciferase-free Luciferin Electrochemiluminescence

M. Belotti, M. M. T. El-Tahawy, L.-J. Yu, I. C. Russell, N. Darwish, M. L. Coote,
M. Garavelli*, S. Ciampi**

Experimental Procedures

Materials. Unless noted otherwise, reagents were of analytical grade and used without further purification. Milli-Q™ water (>18.2 MΩ cm resistivity) was used for surface cleaning procedures and to prepare electrolytic solutions. Luciferin sodium salt was purchased from Cayman Chemical Company (≥95 %, Ann Arbor, Michigan). Adenosine 5'-monophosphate monohydrate (≥97.0%, AMP), *N,N*-dicyclohexylcarbodiimide (DCC, ≥99.0%), tetrabutylammonium perchlorate (Bu₄NClO₄, ≥98.0%), lithium perchlorate (LiClO₄, ≥98.0%), anhydrous dimethyl sulfoxide (DMSO, ≥99.9%), tetrahydrofuran (THF, ≥99.0%, anhydrous, with 250 ppm of butylated hydroxytoluene as inhibitor), potassium dioxide (KO₂, ≥95%), and D-luciferin ethyl ester (≥97.5%) were purchased from Sigma. Pyridine (≥99.5%, Honeywell, Charlotte, North Carolina), *N,N*-dimethylformamide (DMF, 99.9%) was purchased from VWR Chemicals (Pennsylvania), and tetrabutylammonium nitrate (Bu₄NNO₃, 97%), tetrabutylammonium hexafluorophosphate (Bu₄NPF₆, 98%), sodium tetrakis[3,5-bis(trifluoromethyl)phenyl]borate (NaBARF, 97%) were purchased from Alfa Aesar. Sodium perchlorate monohydrate (NaClO₄·H₂O, 90.0%) was purchased from Univar. Argon (Ar, >99.999%) and oxygen gas (O₂, ≥ 99.5%) were supplied from Coregas. Deuterated DMSO (d₆-DMSO, 99.5%) was purchased from Cambridge Isotope Laboratories, Inc.

Synthetic procedures. Firefly luciferyl adenylate (**AMP-luc**) was prepared according to the procedure of White and co-workers (Figure S18).^[1] In brief, luciferin sodium salt (0.33×10^{-3} mol) and AMP (0.37×10^{-3} mol) were dissolved in pyridine (~5.0 mL), then the solution was acidified with 0.5 M aqueous hydrochloric acid (0.5 mL). DCC (0.63×10^{-3} mol) in pyridine (~2.0 mL) was added in one portion, under nitrogen, to the stirred and ice-cold reaction mixture. The reaction mixture was stirred under nitrogen at 0 °C for a further 30 min. Cold acetone (~20 mL, -20 °C, containing) was then added to the crude reaction mixture in one portion. A pale yellow precipitate formed and was recovered by filtration on 0.45 μm nylon filters (BaseLine Chromtech). The solid was washed extensively with cold acetone (~100 mL, cold acetone containing ~5.0% v/v of water). The **AMP-luc** yellow powder product was dried under vacuum, then stored at -20 °C under argon prior to use. ¹H NMR (400 MHz, DMSO-d₆) δ 9.55 (1 H, s), 8.39 (1 H, s), 8.16 (1 H, s), 7.96 (1 H, d, 9 Hz), 7.46 (1 H, d, 3 Hz), 7.28 (2 H, s), 7.08 (1 H, dd, 9 Hz, 3 Hz), 5.93 (1 H, d, 6 Hz), 5.46 (1 H, t, 9 Hz), 4.62 (1 H, t, 5 Hz), 4.21 (1 H, dd, 5 Hz, 3 Hz), 4.07 (1 H, br. s), 4.05 (1 H, br. s), 3.94 (3 H, m), 3.75 (1 H, dd, 11 Hz, 9 Hz), 3.66 (1 H, dd, 11 Hz, 9 Hz). **AMP-luc** purity was estimated by titrating the reaction product with aqueous sodium hydroxide. The electrolyte/**AMP-luc** solution was placed in an optical glass rectangular cuvette (40 × 10 × 45 mm, part 3/G/40, Starna, Hainault) with the largest face facing a focusing lens (LA4647, Thorlabs) interfaced with an optical fiber (Model QP600-1-SR, Ocean Optics) connected to a compact silicon CCD array spectrometer (Flame-S-VIS-NIR-ES, Ocean Optics Inc., Orlando, Florida). The cuvette was fitted with a three electrodes system as described in the next section (spectroelectrochemical measurements). The titration was performed inside a light-proof metal box. The titration procedure was as follows: sodium hydroxide solution (2.0×10^{-3} M) was added dropwise to 9 mL of a vigorously stirred **AMP-luc** solution (0.2 g/L) in 0.2 M Bu₄NClO₄/DMSO. **AMP-luc** is progressively consumed in a stoichiometric reaction with sodium hydroxide.^[2] The emission intensity in response to the electrochemically triggered light emission from the residual, unreacted **AMP-luc** (working electrode bias set to -2.0 V) was monitored continuously, allowing a short interval (1 min) between successive additions of the base. When all **AMP-luc** is consumed, light emission ceases and this is the titration endpoint. The amount of **AMP-luc** present in the crude reaction product ranged from 55% to 75% w/w (and the reaction yield ranged from 32% to 47%).

Spectroelectrochemical measurements. All spectroelectrochemical measurements were acquired with freshly made solutions of **AMP-luc** (0.43×10^{-3} M) in DMSO, with either Bu₄NClO₄ (0.2 M), Bu₄NNO₃ (0.2 M), Bu₄NPF₆ (0.2 M), LiClO₄ (2.0 M, 0.2 M and 5.0×10^{-3} M) NaClO₄ (0.2 M), and NaBARF (0.2 M) as electrolytes, or in THF with LiClO₄ (0.2 M and 5.0×10^{-3} M) or NaBARF (0.05 M), or in DMF with Bu₄NClO₄ (0.2 M). Unless specified otherwise, oxygen gas (≥99.95%, Coregas) was bubbled through the **AMP-luc** solution (~20 mL) for at least 20 min prior to the experiments. Spectroelectrochemical measurements were carried out under ambient air, at room temperature, using an Emstat3 Blue potentiostat (PalmSens BV, Houten, Netherlands) and a single-compartment, three-electrode setup. A platinum rectangular mesh (7 × 6 mm overall size) served as the working electrode (EF-1355 SEC-C Gauze, 80 mesh, wire diameter of 80 μm, BASi, Lafayette, Indiana), a platinum coil as counter electrode, and a leakless Ag|AgCl as the reference electrode (ET072-1, eDAQ, Colorado Springs, Colorado, 3.4 M aqueous potassium chloride as filling solution). The spectroelectrochemical cell was a quartz cuvette of 0.5 mm optical length (EF-1364 SEC-C, BASi), fitted with a perforated PTFE cap was holding up the electrodes (EF-1359 SEC-C). Light emission was recorded with a Cary Eclipse (Varian, Palo Alto, California) fluorescence spectrophotometer operated in Bio/Chemi-luminescence mode. The photomultiplier voltage was set to 800 V, and unless specified otherwise, the emission slit was set to 5 nm for experiments in DMSO, and to 20 nm for experiments in THF. Platinum electrodes were cleaned prior to the experiments by continuous potential cycling between -0.2 and 1.0 V (0.5 M HNO₃, 0.01 V s⁻¹).

Photon Counting. Photon counting experiments were performed with a single-photon counting module (SPCM-AQR-14, Excelitas Technologies) interfaced with an avalanche photo-diode (APD) controller (Nanonics Imaging Ltd., Figure S19). The photon counts rate output of the APD controller was monitored with a data logger (DrDAQ, Pico Technology). The time constant of the APD counter was set to 1.0 ms. The electrochemical setup is the one described in the previous section, and light emission was measured from a 0.43×10^{-3} M solution of **AMP-luc** in DMSO, containing 0.2 M Bu₄NClO₄ as supporting electrolyte, and with the platinum mesh working electrode bias ramped from 0.0 V to -2.0 V. The photon counts rate was corrected for the nominal wavelength-dependent efficiency of the counting module (ca. 70% at 625 nm). The 99% confidence limit of the mean photon counts value is reported as $t_{n-1}s/n^{1/2}$, where t_{n-1} is 3.05, s is the standard deviation, and n the number of repeated measurements (13).^[3]

SUPPORTING INFORMATION

Luminescence imaging. Time-resolved chemiluminescence images were recorded on a Nikon Eclipse Ti2-U inverted microscope fitted with a custom-built optoelectrochemical cell (Figure S20a) and using either a Plan Apo λ 4 \times /0.45 objective (part 88-378, Nikon, CFI Plan Fluor) or a Plan Apo λ 10 \times /0.45 objective (part 88-379, Nikon, CFI Plan Fluor). As for the spectroelectrochemical measurements, the electrolytic solution (**AMP-luc**, 0.43×10^{-3} M in 0.2 M Bu₄NClO₄/DMSO) was oxygen saturated, and loaded in a glass Petri dish mounted on the microscope holder. Light emission was triggered by applying -2.0 V vs Ag/AgCl to a platinum mesh working electrode. The electrochemical set up is analogous to the one described above for the spectroelectrochemical measurements, with the difference that the single-compartment electrochemical cell is made up from the petri dish and a PTFE holder designed to hold the working electrode's main face normal to the microscope objective axis (Figure S20b–c). Prior to the experiments, platinum electrodes were cleaned by continuous potential cycling as described above. Cathodic electrolysis of the **AMP-luc** solution leads to a transient light emission whose front diffuses away from the electrode surface. Time-resolved imaging of the **AMP-luc** electrochemically generated emission was performed with a colour camera (DS-Fi3, Nikon, Tokyo, Japan) without any filtering nor any excitation light, and using either 1.0 s (Figure 1c, Video S1) or 500 ms (Figure 4a–c, Video S2) exposure time. The gain set to its maximum for the shorter exposures. All microscopy images were analyzed with the Fiji image processing package.^[4] Diffusivities were estimated by analyzing the profile of the red electrochemiluminescence intensity along the surface normal direction, as function of time after the initial cathodic potential pulse. Time-stamped light-intensity line profiles were used to estimate the distance from the electrode (r) at which the intensity reaches half of its maximum value. This distance was arbitrarily defined as the diffusion front. Images were not background subtracted, and for this analysis no attempts were made to improve contrast and sharpness (e.g. unmodified Videos S1 and S2). Line profiles such as those of Figure 4a–c of the main text are measured along a direction normal to the electrode surface, with point A being generally within 1–3 μ m from the electrode surface. The diffusion coefficient was calculated assuming an Einstein's random walk ($r^2 = 2Dt$).^[5] This procedure was repeated for 2 different videos, with at least 10 different locations sampled in each video. The 99% confidence limit of the mean photon counts value is reported as $t_{n-1}s/n^{1/2}$, where t_{n-1} is 2.68, s is the standard deviation and n the number of measurements (48).^[3] Electrochemiluminescence images shown in Figure 2 (main text) were recorded using a CMOS camera (CS235CU, Thorlabs) fitted with a machine-vision lens (MVL50M23, Thorlabs, 50 mm, f/2.8). Selected video frames reproduced in Figure 4a–c of the main text have been background subtracted for clarity (Fiji).

Fluorescence imaging. The electrochemical conversion of **AMP-luc** to **ox-luc** can be used to map optically diffusivities. Unlike the electrolysis' starting material (**AMP-luc**), the product of the electroluminescent reaction, **ox-luc**, is fluorescent.^[6] The procedure for the in-situ optical mapping of diffusivities was similar to that reported above for the electroluminescence imaging and consisted in the analysis of the distance (r) travelled over time by the fluorescence front, away from the electrode surface and along the A–B line marked in Figure S17. Time-lapsed fluorescence emission images for the excitation of the electrochemically generated **ox-luc** were recorded with a CMOS monochrome camera (DS-Qi2, Nikon) using a 20 ms exposure time. Excitation and emission light were defined by a FITC filter/dichroic mirror cube (LED-FITC-A-NTF-ZERO, excitation filter part number FF01-474/27-25, emission filter part number FF01-525/45-25, dichroic mirror part number FF495-Di03-25x36, BrightLine®, Semrock, Illinois). The obtained "optical" D values are in line with what can be obtained by established electrochemical methods for molecules of similar molecular weight, such as methyl viologen.^[7]

Theoretical calculations. To determine a reaction the mechanism, density functional theory (DFT) and time-dependent DFT (TD-DFT) calculations were performed using Gaussian 16 revision C.01.^[8] Geometry optimizations and frequency calculations were performed at the M062X/6-31+G(d,p) level of theory in the presence of DMSO, which was modelled using the SMD continuum solvent model.^[9] All structures were conformationally searched using the Energy Directed Tree Search (EDTS) algorithm,^[10] and all transition states were confirmed using Intrinsic Reaction Coordinate (IRC) calculations. Improved single point energies in solution were calculated using the ω B97XD functional with the Def2TZVP basis set with the SMD solvent model.^[11] Gibbs free energies were calculated using the direct method,^[12] whereby ideal gas partition functions were evaluated using the solution-phase geometries and frequencies. The conversion ($RT\ln(RT/P)$) from the gas-phase standard state of $P = 1.0$ atm used in the partition function calculations to the solution-phase standard of 1.0 M was added to the final Gibbs free energies.^[13] pKa values (298 K, DMSO) were computed via an isodesmic method using 4-hydroxydinaphtho[2,1-d:1',2'-f][1,3,2]dioxaphosphepine 4-oxide (experimental pKa = 3.37^[14]) as a reference.

To determine the spectral tuning, excited state computations were performed employing QM and QM/MM calculations for vacuum and explicit solvents (THF and DMSO), respectively. The initial geometries of the luciferin for Quantum Mechanics/Molecular Mechanics (QM/MM) calculations in the explicit solvents were selected from MD snapshots of Classical MM simulations of keto-form in both dimethyl sulfoxide (DMSO) and tetrahydrofuran (THF) solvents. The MM simulations were performed via Amber-18 suite employing ff10 force field.^[15] We used DFT-B3LYP/6-311++G(p,d)^[16] with the IEFPCM implicit solvent model,^[17] GAFF force field^[18] and RESP charges to parameterize the nonstandard residues in DMSO and THF. The keto form is solvated with an octahedral solvent box of 18 Å solvent molecules via standard amber tools techniques. The force fields of DMSO and THF molecules were parameterized as reported by Fox and Kollman method,^[19] while the RESP method reported by Dupradeau et al.^[20] is used to assign their atomic charges. The solvated systems were then pre-equilibrated at constant volume and temperature, heating from 0 to 300 K, and then a 20-ns molecular dynamic simulation run was performed at constant temperature (300 K) and pressure (1atm) using Berendsen barostat as implemented in Amber-18.^[21] A cluster analysis performed over the snapshots extracted every 100 fs from the equilibrated system trajectory; then the snapshots characterized by highest populations and the lowest potential energies were extracted to be used as starting structures for the subsequent QM/MM calculations. Only solvent molecules within a 15Å distance from the keto-form atoms were eventually considered in defining the solvation shells around the solutes in the following QM/MM computations.

SUPPORTING INFORMATION

To carry out the QM/MM calculation in DMSO and THF, a three-layer HML scheme has been designed through COBRAMM package,^[22] where the QM region (high layer, H) involves the keto or the enol forms (enol form was adapted from the keto form snapshot after shifting the H atom from C₅ to O₁₁), the surrounding solvent molecules that are 5Å apart were left free to move (medium layer, M), and the remaining solvent molecules were kept frozen at their snapshot coordinates (low layer, L). The keto and enol forms were treated quantum mechanically using the complete active space self-consistent field (CASSCF) level of theory as follows, while solvent molecules were described by the AMBER force field. The QM calculations were carried out using Molcas 8 as implemented in the QM/MM COBRAMM package employing an electrostatic embedding scheme.^[22-23] The S₁ excited-state geometries of the luciferin fluorophores (keto- and enol-forms) were optimized using unconstrained optimizations employing the complete active space self-consistent field (CASSCF) level of theory^[24] with ANO-S-VDZP basis set^[25] and averaging over the first two roots. In all the calculations and in agreement with our studies in different environment,^[26] the ionization-potential-electron-affinity shift^[27] was fixed at 0.0 au while the value 0.2 au was chosen for the imaginary shift.^[28] An active space (AS) including 16 electrons distributed in 14 orbitals CAS(16,14) was used for optimizations, while the extended multistate second order perturbation correction method (XMS-CASPT2) was employed on top of the excited state optimized geometries to account for correlation energy and get experimentally accurate estimates of the emission spectra. An extended AS comprising 18 electrons in 15 orbitals, CAS (18, 15), was used in this case (Figures S21 and S22) by averaging over the first two (SA-2) roots.^[29] Computations in the presence of an external linear homogeneous electric field in the Z-direction were performed using the FFPT module as incorporated in Molcas. All the structures have been re-optimized using the CASSCF gradients under the effect of an external homogenous electric field in each environment, employing Molcas and the QM/MM COBRAMM code. Applying the electric field along the z-direction this direction is associated with both direction of the charge transfer and the direction of the dipole moment change upon S₁→S₀ transition (see Figure S11) consequently a maximum effect on the emission spectra is shown with applying the electric field in this direction.

Supporting Figures

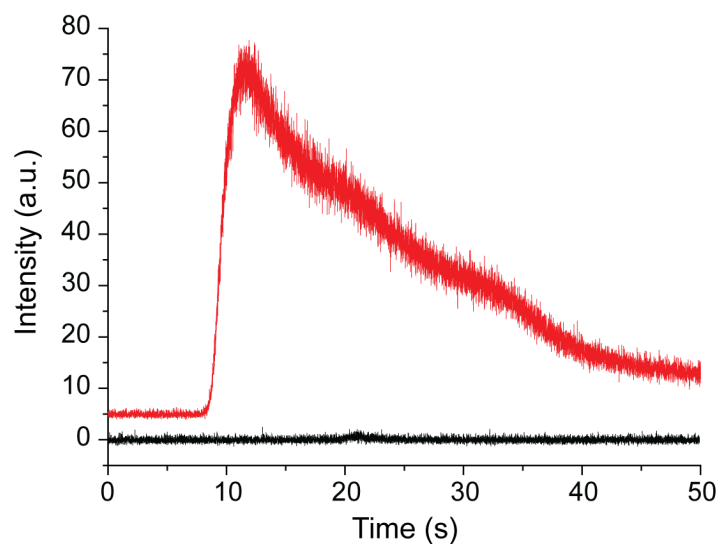


Figure S1. Time-evolution of the electrochemically generated light emission upon the electrolysis of **AMP-luc** (0.43×10^{-3} M in 0.2 M $\text{Bu}_4\text{NClO}_4/\text{DMSO}$) at a platinum mesh electrode. The electrolytic solution was either oxygen-saturated (red trace), or argon-saturated (black trace). The voltage of the working electrode was ramped from 0.0 V to -2.0 V (and back, one cycle) at a scan rate of 0.1 V/s. The electrochemiluminescence was monitored at 626 nm (emission slit set to 2.5 nm). The red trace is vertically offset by 5 a.u. for clarity purposes.

SUPPORTING INFORMATION

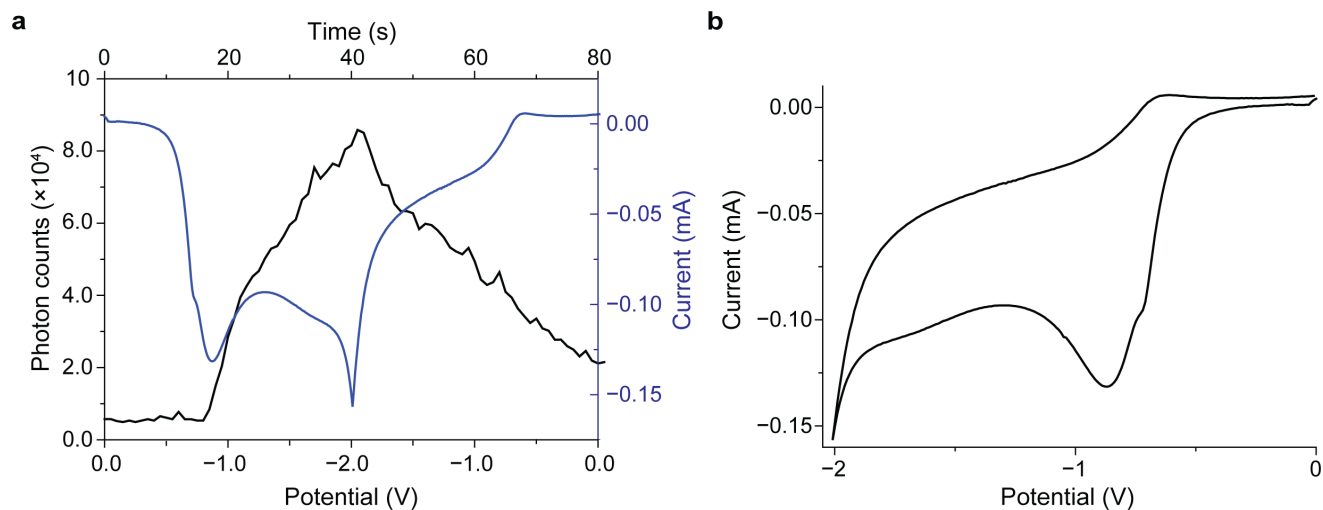


Figure S2. (a) Representative simultaneous photon counting and current recording for the electrochemically generated light emission from the electrolysis of an oxygen-saturated **AMP-luc** solution (0.43×10^{-3} M in 0.2 M $\text{Bu}_4\text{NClO}_4/\text{DMSO}$) at a platinum mesh electrode. (b) The electrode potential was swept cyclically between 0.0 V (starting point) and -2.0 V at a voltage sweep rate of 0.05 V/s. The emission peak corresponds to $\sim 8.5 \times 10^4$ photon/s.

SUPPORTING INFORMATION

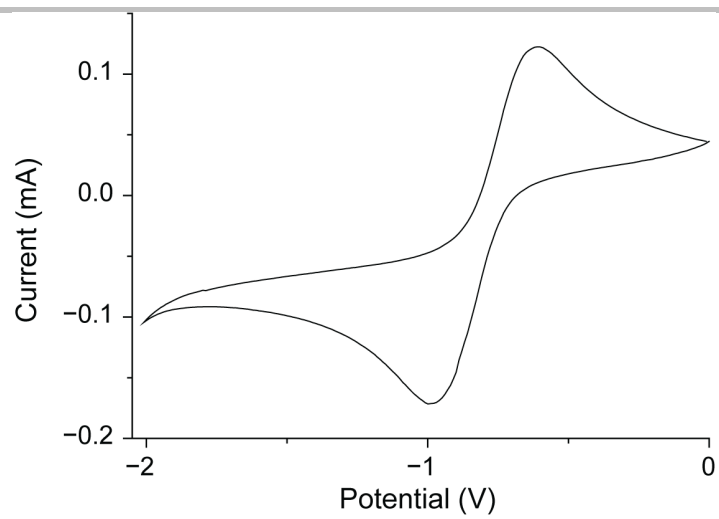


Figure S3. Representative cyclic voltammogram (CV) recorded at a platinum mesh electrode in oxygen-saturated 0.2 M Bu₄NClO₄/DMSO (without **AMP-luc**). The voltage scan rate is 0.05 V/s.

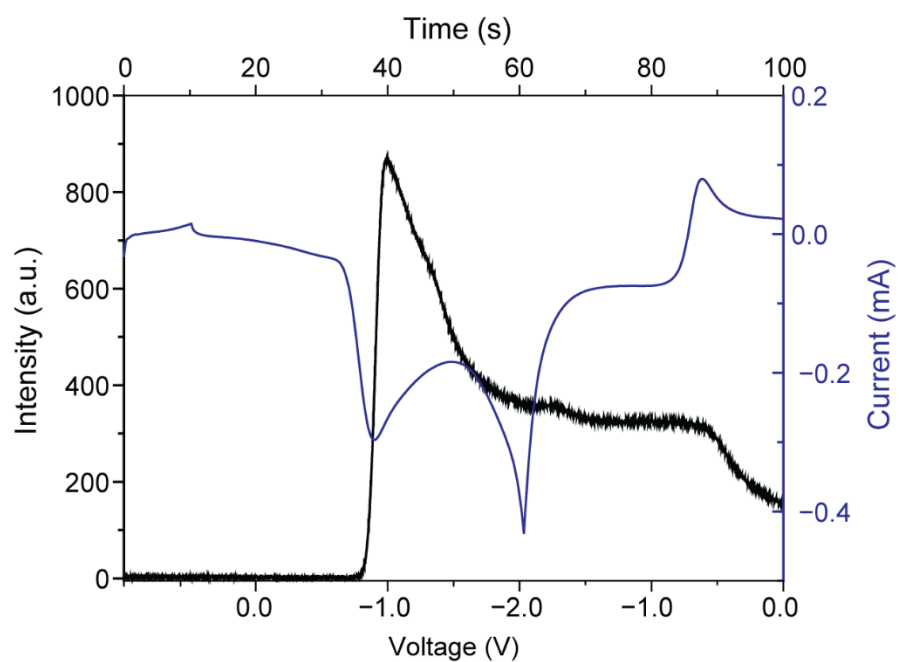


Figure S4. Time-evolution of the electro-generated emission of an oxygen-saturated **AMP-luc** solution (0.43×10^{-3} M in 0.2 M $\text{Bu}_4\text{NClO}_4/\text{DMSO}$) at a platinum mesh electrode. Light emission was recorded during a cyclic voltammetry (CV) experiment, with the working electrode bias ramped first from 0.0 V to +0.5 V, then from +0.5 V to -2.0 V (and back to 0.0 V). The electrochemiluminescence is monitored at 626 nm (black trace, Cary Eclipse). The potential scan rate was 0.05 V/s and the CV current (blue line) is plotted vs time.

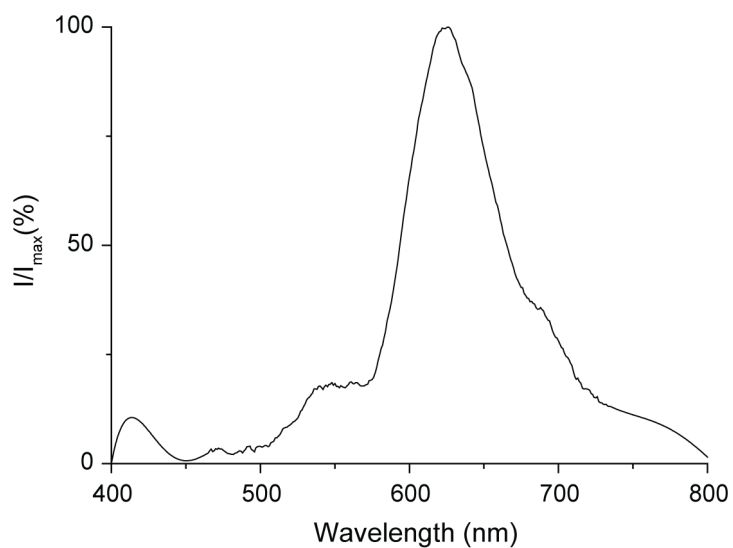


Figure S5. Representative emission spectrum for the cathodic electrolysis of an oxygen-saturated D-luciferin ethyl ester solution (0.5×10^{-3} M) at a platinum mesh electrode. The electrolyte was 0.2 M $\text{Bu}_4\text{NClO}_4/\text{DMSO}$. The working electrode bias is -3.0 V. At -2.5 V the emission was almost undetectable, and at -2.0 V no emission was detectable. The emission slit was set to 20 nm.

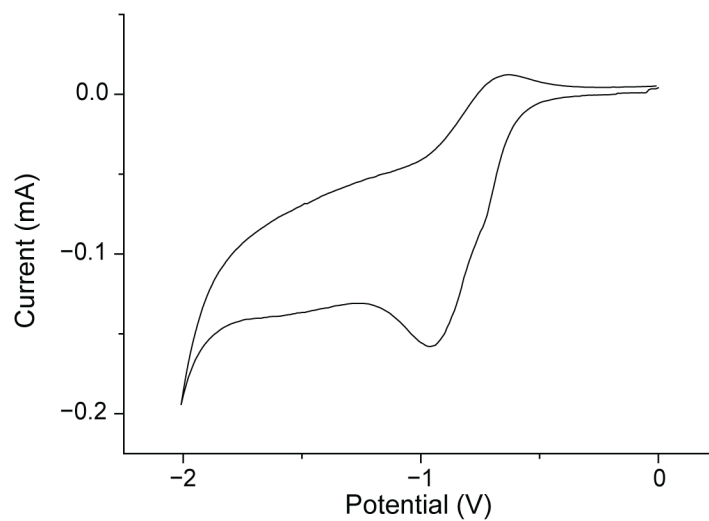


Figure S6. Representative cyclic voltammogram (CV) at a platinum mesh electrode of an **AMP-luc** solution ($\sim 0.43 \times 10^{-3}$ M in oxygen-saturated 0.2 M $\text{Bu}_4\text{NClO}_4/\text{DMSO}$) showing a clear reduction band for the one-electron reduction of oxygen to superoxide. The voltage scan rate is 0.05 V/s.

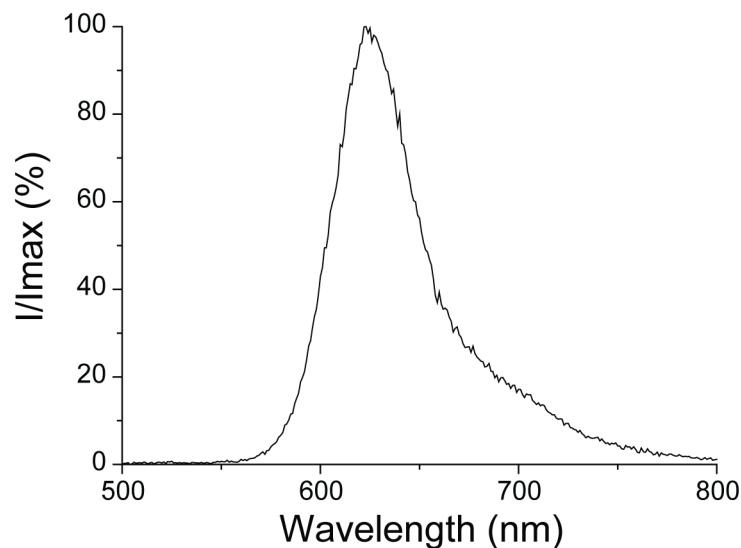


Figure S7. Emission spectrum from an **AMP-luc** solution (0.43×10^{-3} M, 0.2 M $\text{Bu}_4\text{NClO}_4/\text{DMSO}$) added to 0.02 g of KO_2 . The **AMP-luc** solution was bubbled with argon gas for ~20 min prior to the experiment. Full experimental details are in the experimental section, but in brief, a cuvette containing the KO_2 powder was placed in the spectrometer chamber (Carry Eclipse). To ensure no ambient light was reaching the detector, the **AMP-luc** solution (4 mL) was fed in one portion from a plastic syringe to the cuvette through a small tube silicone tubing (3.0 mm diameter). The emission spectra were recorded while the solution was being added to the cuvette (over a period of ~4.0 s), initiating the chemiluminescent reaction. A complete spectrum was recorded in approximately 1.5 s. The spectrometer sample compartment was kept under positive argon gas pressure. The solubility of KO_2 in DMSO is limited.^[30] The addition of the **AMP-luc** solution to the solid KO_2 sample results in a cloudy suspension, and unreacted solid KO_2 is still visible in the cuvette after the spectral measurement.

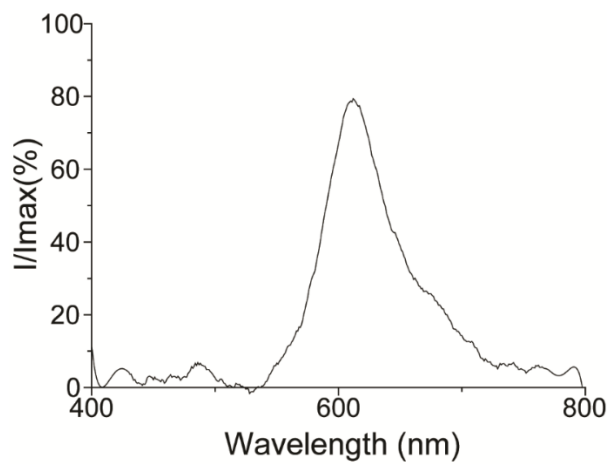


Figure S8. Representative emission spectrum for the cathodic electrolysis of an oxygen saturated **AMP-luc** solution (0.43×10^{-3} M) on a platinum mesh electrode. The electrolyte was 2.0 M LiClO₄ in DMSO. At such high concentrations of LiClO₄, the electrochemically triggered luciferin emission undergoes a blue shift. Data are collected applying a -2.5 V bias to the working electrode.

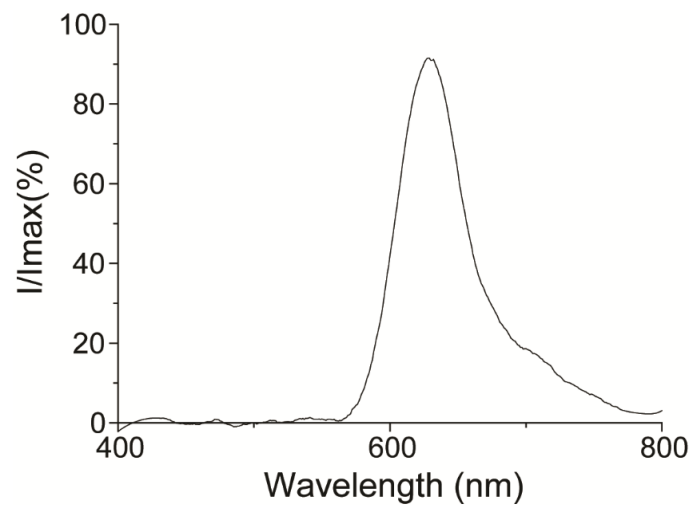


Figure S9. Representative emission spectrum obtained upon the cathodic electrolysis of an oxygen saturated **AMP-luc** solution (0.43×10^{-3} M) at a platinum mesh electrode. The electrolyte was 5.0×10^{-3} M LiClO₄/DMSO. Unlike for THF (Figure 3c, main text), with DMSO there is no shift at very low concentrations of LiClO₄. Data were collected applying -1.5 V to working electrode.

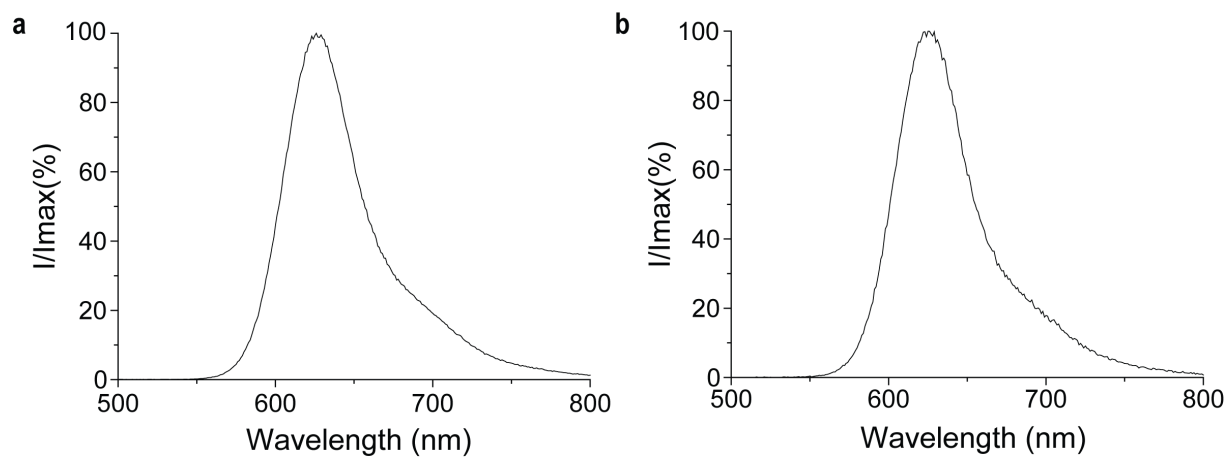


Figure S10. Representative emission spectra for the cathodic electrolysis of oxygen saturated **AMP-luc** solutions (0.43×10^{-3} M) at a platinum mesh electrode. The electrolytes were 0.2 M $\text{Bu}_4\text{NNO}_3/\text{DMSO}$ in (a), and 0.2 M $\text{Bu}_4\text{NPF}_6/\text{DMSO}$ in (b). Changes to the anion have no measurable effect on the energy of the **AMP-luc** electroluminescence. Data were collected applying -2.5 V to the working electrode.

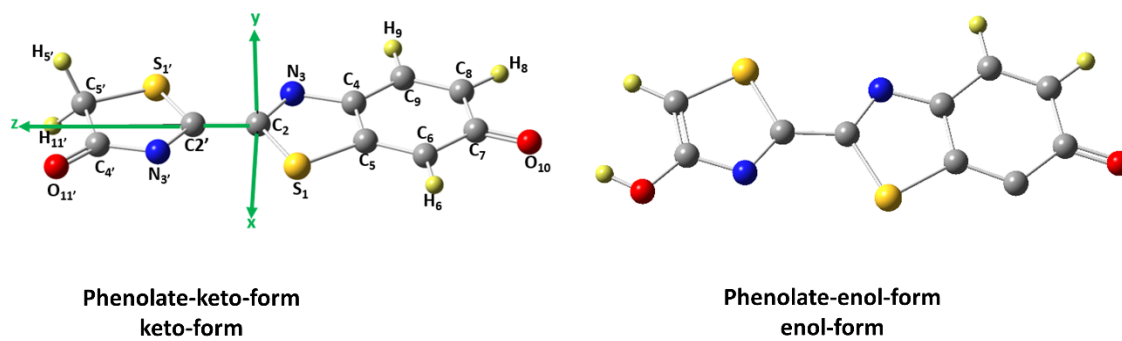


Figure S11. 3D model of the two luciferin isomers. The keto-form is shown on the right, and the enol-form on the left.

SUPPORTING INFORMATION

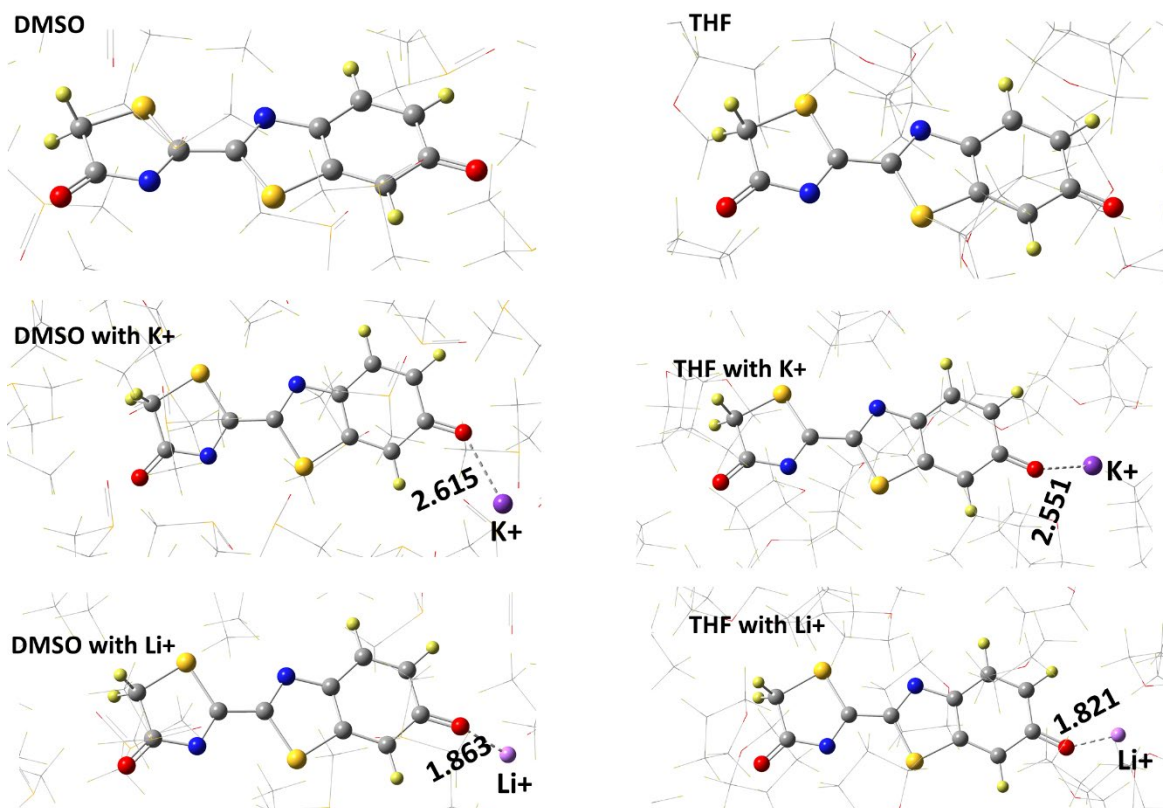


Figure S12. CASSCF optimized structure(s) of the Table 1 excited (emitter) species in molecular mechanics (MM) DMSO (left) and THF (right).

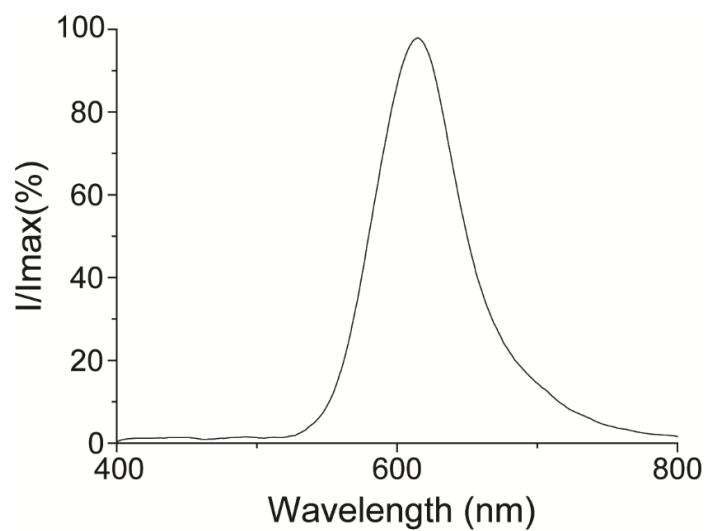


Figure S13. Representative emission spectra for the cathodic electrolysis of an oxygen saturated **AMP-luc** solution (0.43×10^{-3} M) at a platinum mesh electrode. The electrolyte was 0.2 M NaClO₄/THF. Unlike for LiClO₄, with NaClO₄ as electrolyte there is no shift in the **AMP-luc** electrochemiluminescent emission. Data were collected applying -2.0 V to the working electrode.

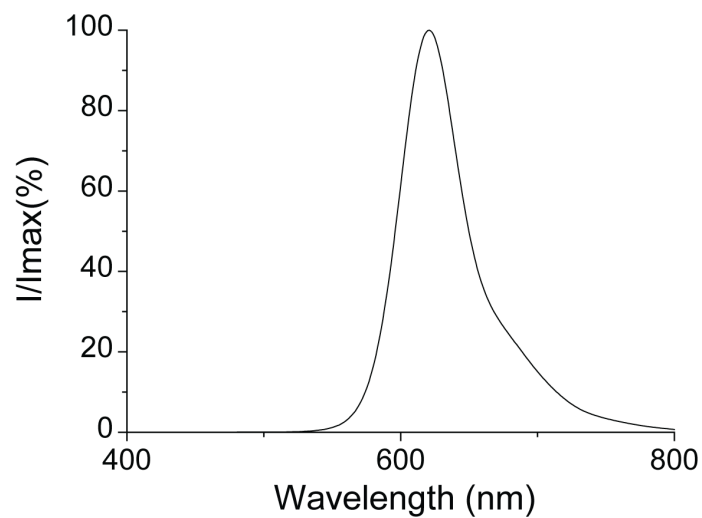


Figure S14. Representative emission spectrum for the cathodic electrolysis of an oxygen saturated **AMP-luc** solution (0.43×10^{-3} M) at a platinum mesh electrode. The electrolyte was 0.2 M $\text{Bu}_4\text{NClO}_4/\text{THF}$. Unlike for LiClO_4 , with Bu_4NClO_4 there is no shift in the **AMP-luc** emission. Data were collected applying -2.0 V to the working electrode.

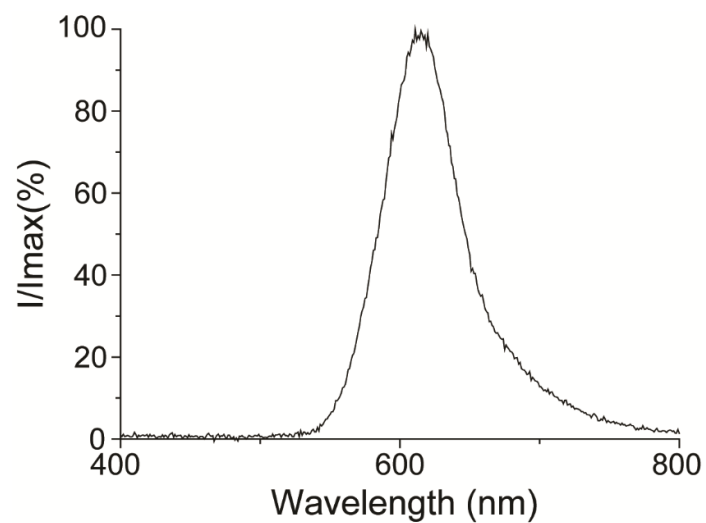


Figure S15. Representative emission spectrum for the cathodic electrolysis of an oxygen saturated **AMP-luc** solution (0.43×10^{-3} M) at a platinum mesh electrode. The electrolyte was 0.05 M NaBARF/THF. Experiments with a completely not-coordinating anion as BARF^- were used to exclude the anion influence on the spectral tuning of the **AMP-luc** electrochemiluminescent emission. Data were collected applying -2.0 V to the working electrode.

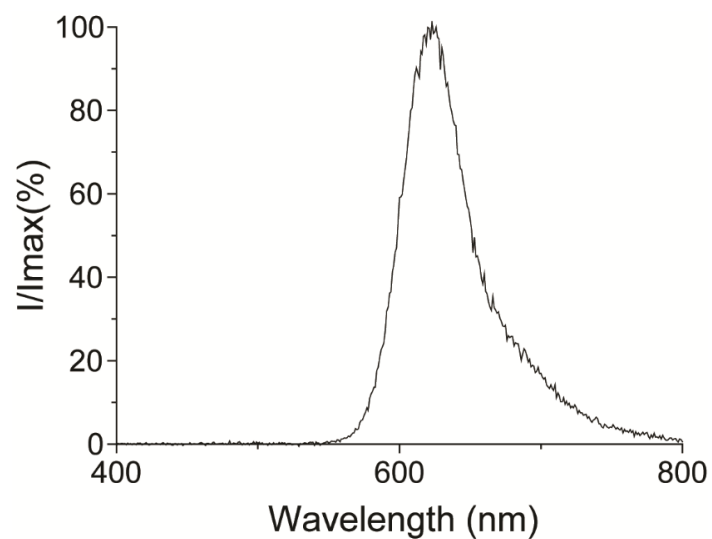


Figure S16. Representative emission spectrum for the cathodic electrolysis of an oxygen saturated **AMP-luc** solution (0.43×10^{-3} M) at a platinum mesh electrode. The electrolyte was 0.2 M $\text{Bu}_4\text{NClO}_4/\text{DMF}$. DMF is a solvent with a high dielectric constant (marginally lower than DMSO), consequently the emission remains in the red. Data was collected applying -2.5 V to the working electrode.

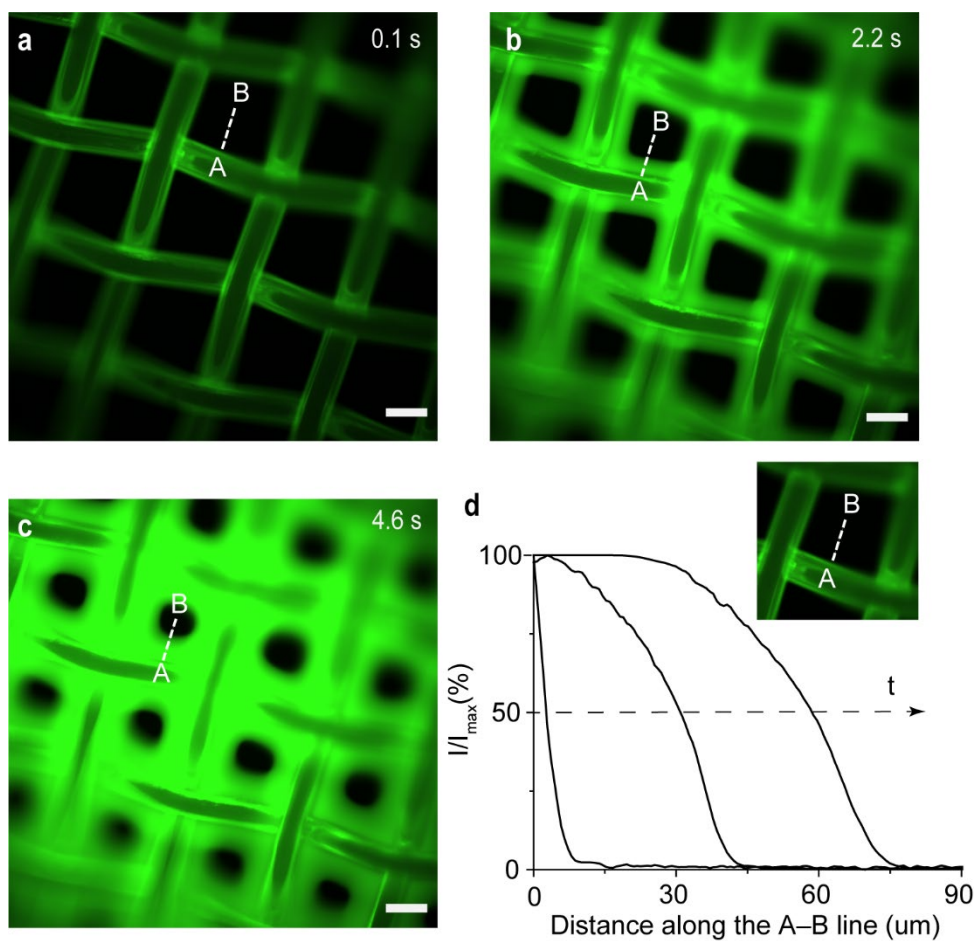


Figure S17. Selected time-stamped images (10 \times magnification) of in-situ generated **ox-luc** fluorescence (474 nm, excitation; 525 nm emission, Video S3), recorded during the electrolysis of an oxygen-saturated **AMP-luc** solution (0.43×10^{-3} M in 2.0×10^{-1} M $\text{Bu}_4\text{NClO}_4/\text{DMSO}$). The fluorescence micrographs were captured under ambient air in a dark room at 0.1 s (a), 2.2 s (b) and 4.6 s (c) after the onset of the cathodic bias voltage (-2.0 V). Scale bars in (a–c) are 100 μm . (d) Selected fluorescence profiles sampled along the A–B line marked in (a–c) and in the panel inset, capturing the movement of the **ox-luc** diffusion front, away from the electrode's surface, at electrolysis times (t) ranging between 0.1 and 4.6 s. The three thicker lines are the fluorescence intensity profiles for the time-stamped images in (a–c). By modelling diffusivity as an Einstein's random walk ($r^2 = 2Dt$), we were able to estimate the **ox-luc** diffusivity (D) to 3.3×10^{-6} $\text{cm}^2 \text{s}^{-1}$.

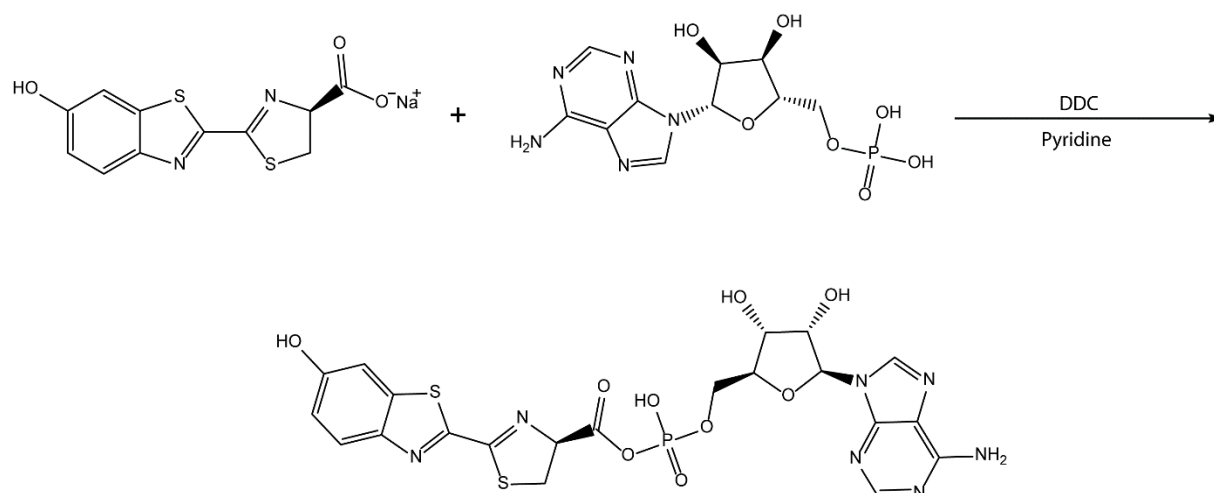
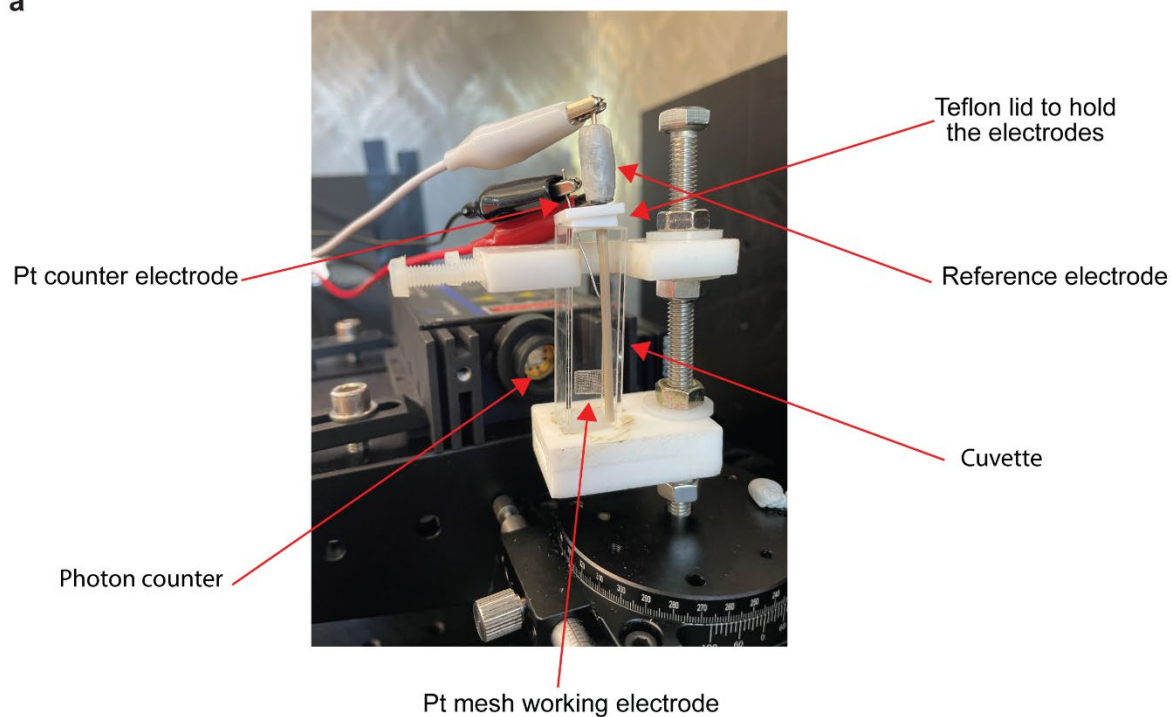


Figure S18. Synthetic scheme for the preparation of **AMP-luc** from luciferin sodium salt and adenosine monophosphate.

SUPPORTING INFORMATION

a



b

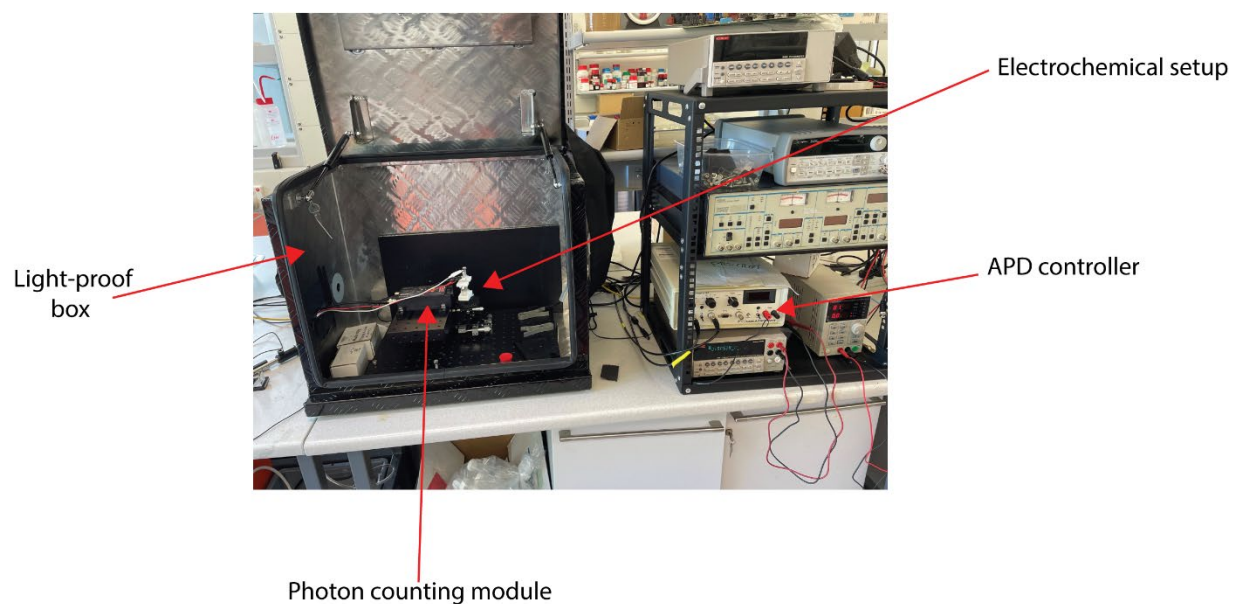


Figure S19. Experimental setup used for the photon-counting (quantitative) electrochemiluminescence experiments. (a) The cuvette containing the electrolytic solution and the three electrodes is placed in front of the counting module using a xyz stage for ensuring consistent positioning of the working electrode (a Pt mesh) relative to the photon counter. Further details in the experimental. (b) Overall view of the experimental apparatus. When the light-proof box is sealed, the dark count approaches 500 photon/s.

SUPPORTING INFORMATION

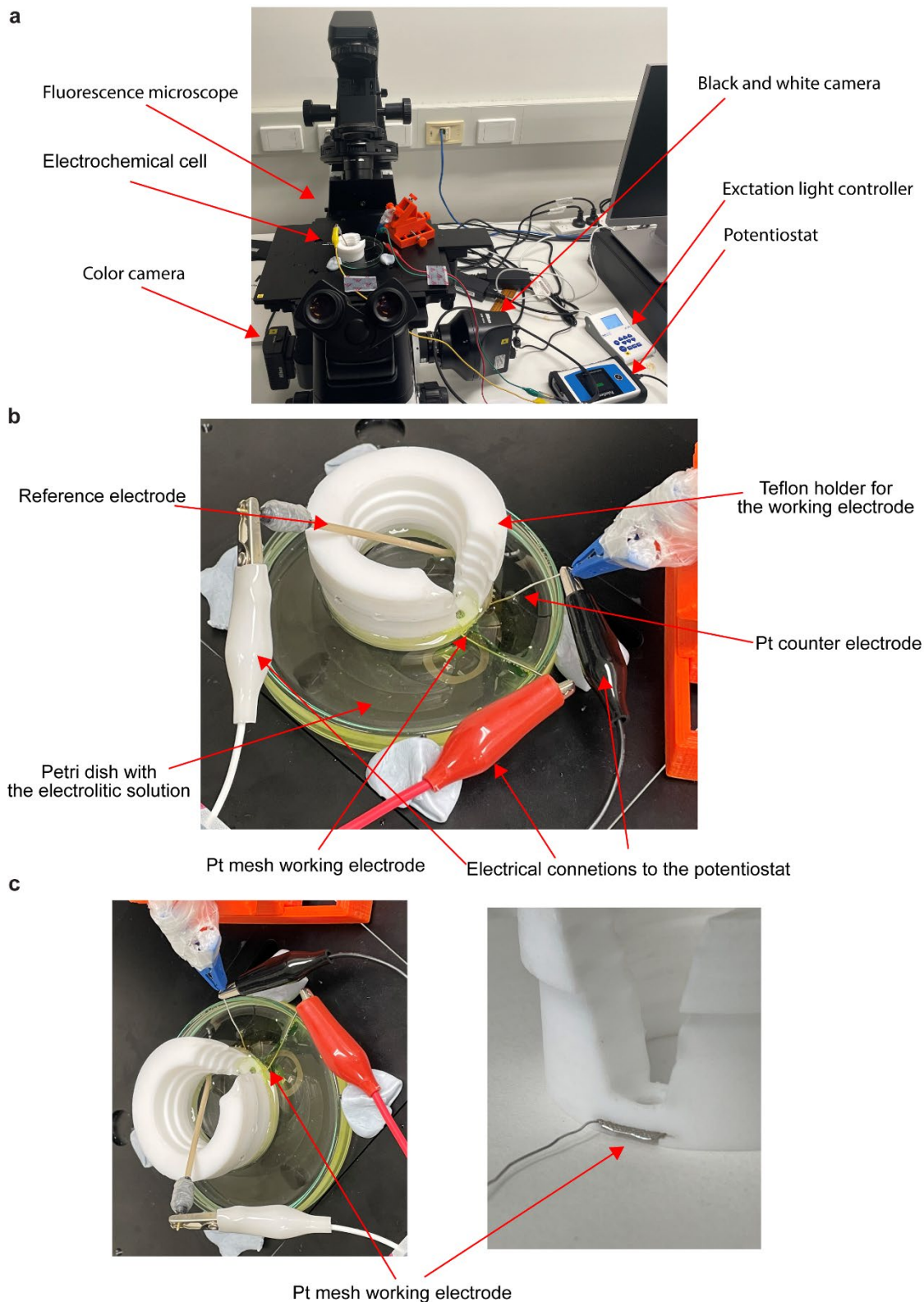


Figure S20. (a) Overview of the experimental setup for the collection of emission (electrochemiluminescence) and fluorescence time-resolved images. (b) A custom electrochemical cell was placed inside a Petri dish resting on the stage of an inverted microscope. The **AMP-luc** solution undergoing electrolysis was placed in the Petri dish. (c) A PTFE holder held the platinum mesh (working electrode) parallel to the Petri dish surface (~2 mm away from it). The electrolytic solution could reach the working electrode both from above (through a rounded hole) and below (opening clearly visible in figure). Further experimental details are in the experimental section.

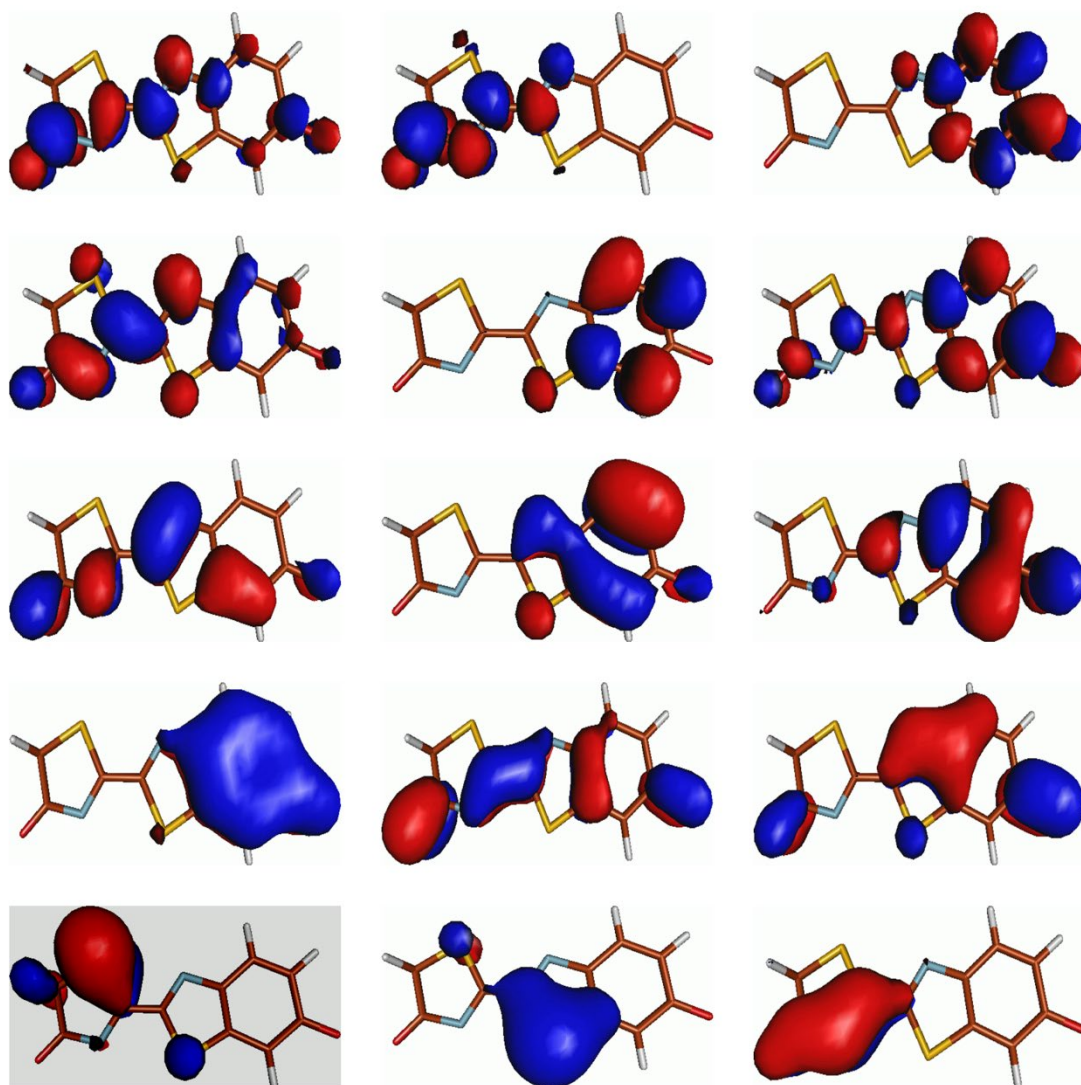


Figure S21. Active orbitals for the CAS(18,15) used in single point calculations for the keto form, the orbital shaded in gray is excluded to adapt CAS(16,14) for geometry optimization calculations. Orbitals are arranged from left to right and bottom to top descending according to the occupation number.

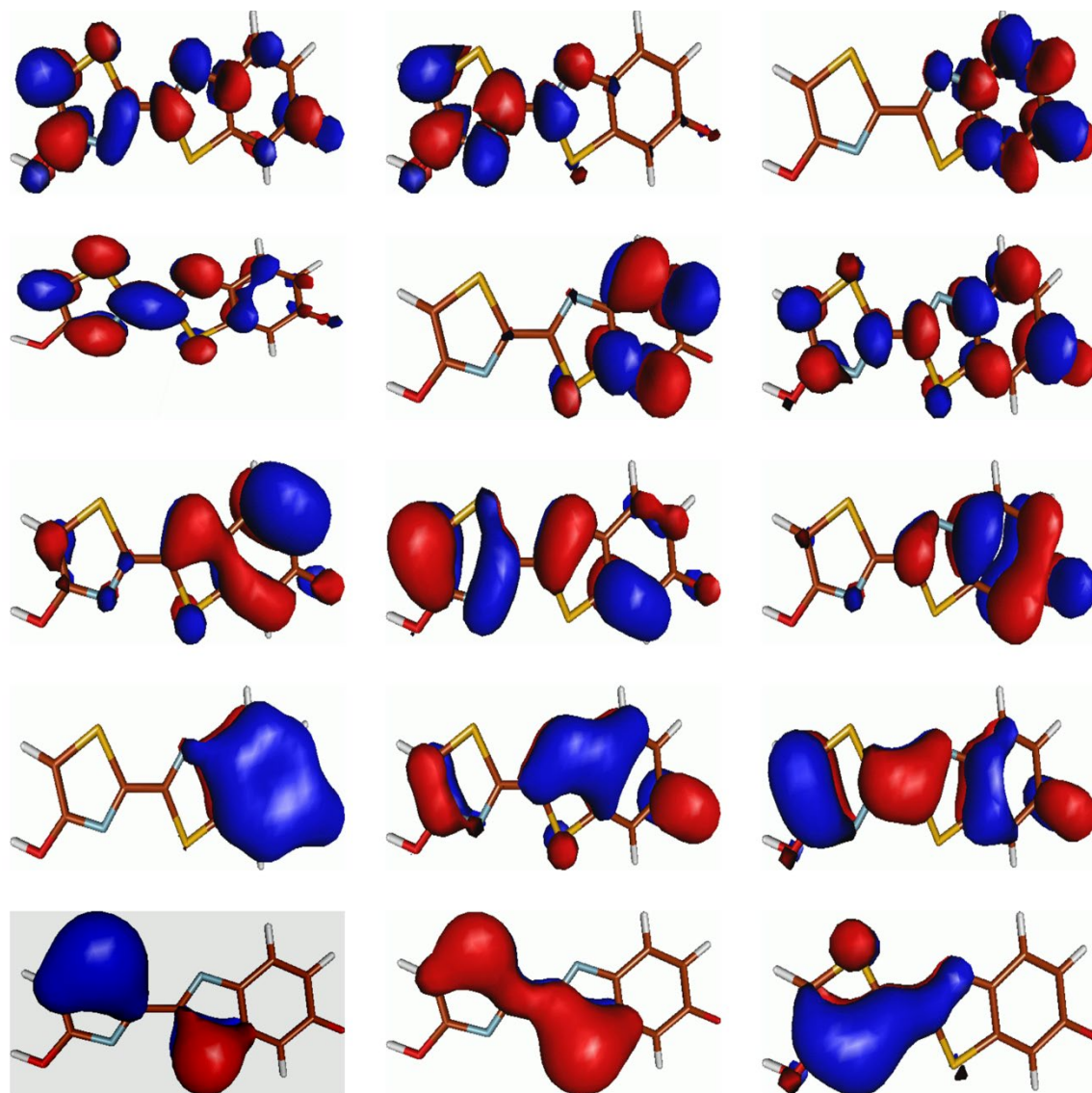


Figure S22. Active orbitals for the CAS(18,15) used in single point calculations for the enol form, the orbital shaded in gray is excluded to adapt CAS(16,14) for geometry optimization calculations. Orbitals are arranged from left to right and bottom to top descending according to the occupation number.

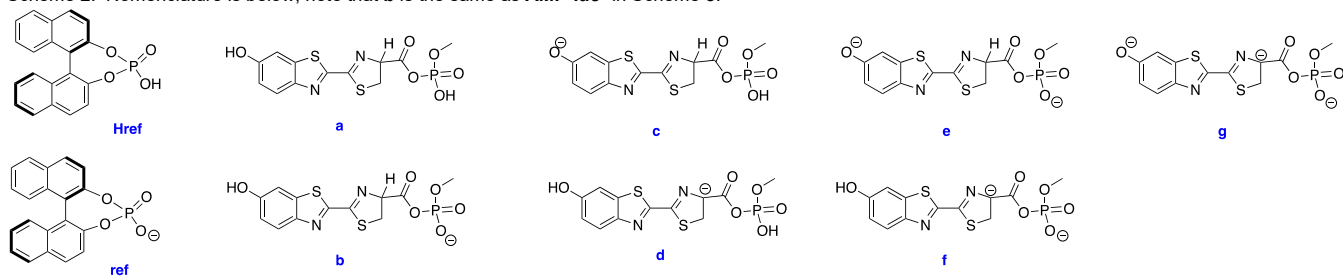
SUPPORTING INFORMATION

Supporting Tables

Table S1. The emission maxima (λ_{max} in nm) of keto-form and enol-form computed at XMS-CASPT2 level of theory in different environments.

	Vacuum	DMSO	DMSO-K ⁺ ion-pair	DMSO-Li ⁺ ion- pair	THF	THF-K ⁺ ion- pair	THF-Li ⁺ ion-pair	
	Emission Maximums (λ_{max})							
Enol	611	574	554	533	584	558	518	
Keto	660	633	603	584	639	608	578	
Exp		625						575
high conc.		610-615						610
	Relative Energy (kJ/mol)							
Enol	67.4	56.5	86.2	86.6	60.7	63.2	68.6	
Keto	0	0	0	0	0	0	0	
	CT							
Enol	-0.27	-0.26	-0.28	-0.28	-0.27	-0.30	-0.27	
Keto	-0.18	-0.20	-0.27	-0.25	-0.21	-0.26	-0.28	

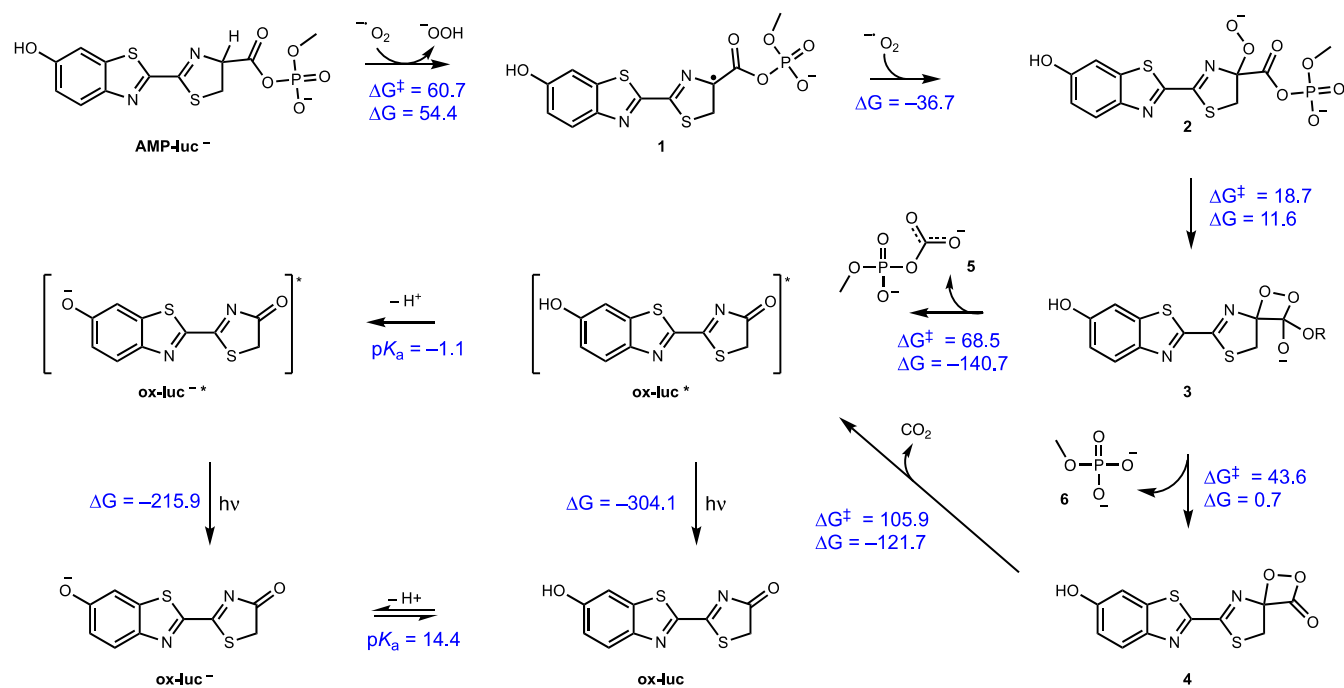
SUPPORTING INFORMATION

Table S2. Gaussian raw data (in a.u., otherwise indicated) and the value of imaginary frequencies (iFreq) for the species use to compute the pK_a values in Scheme 2. Nomenclature is below; note that **b** is the same as **AMP-luc⁻** in Scheme 3.

Species	iFreq	Ee	ZPVE	TC	S(J mol ⁻¹ K ⁻¹)	TS	H	Ee(high)	G_corrected ^a
Href	N/A	-1411.946770	0.285739	0.019266	574.325373	0.065220	-1411.641765	-1412.422039	-1412.179245
ref	N/A	-1411.500551	0.274459	0.018694	564.180896	0.064068	-1411.207398	-1411.967450	-1411.735357
a	N/A	-2162.163981	0.235581	0.022912	684.611343	0.077744	-2161.905488	-2162.744440	-2162.560681
b	N/A	-2161.716635	0.224026	0.022416	678.306269	0.077028	-2161.470193	-2162.288971	-2162.119557
c	N/A	-2161.685728	0.221768	0.022823	683.854030	0.077658	-2161.441137	-2162.258748	-2162.088806
d	N/A	-2161.690944	0.221323	0.022947	676.131194	0.076781	-2161.446673	-2162.259660	-2162.089162
e	N/A	-2161.236871	0.210547	0.022167	673.559851	0.076489	-2161.004157	-2161.801718	-2161.642484
f	N/A	-2161.229334	0.209396	0.022515	670.336866	0.076123	-2160.997423	-2161.789833	-2161.631035
g	N/A	-2160.739142	0.196211	0.022164	664.480896	0.075458	-2160.520767	-2161.291730	-2161.145804

^aAfter adding phase change correction term to the Gibbs free energy

SUPPORTING INFORMATION

Table S3. Gaussian raw data (in a.u. unless otherwise indicated) and number of imaginary frequencies (NImag) for the species use to compute the Gibbs free energy barriers and reaction energies in Scheme 3. The nomenclature is defined in Scheme 3, which is reproduced here for convenience.

Species	iFreq	Ee	ZPVE	TC	S(J mol ⁻¹ K ⁻¹)	TS	H	Ee(high)	G_corrected ^a
CO ₂	N/A	-188.518140	0.011747	0.003578	213.808955	0.024280	-188.502815	-188.607090	-188.616045
O ₂ ^{••}	N/A	-150.388339	0.002967	0.003315	203.197761	0.023075	-150.382057	-150.453385	-150.470177
HOO-	N/A	-150.992777	0.013701	0.003839	225.054179	0.025557	-150.975237	-151.055559	-151.063576
H ₂ O ₂	N/A	-151.502184	0.026079	0.003825	228.365224	0.025933	-151.472280	-151.581668	-151.577697
5	N/A	-870.909434	0.068772	0.010098	401.728358	0.045620	-870.830564	-871.209630	-871.176380
6	N/A	-682.354516	0.053812	0.007448	344.128507	0.039079	-682.293256	-682.573549	-682.551368
AMP-luc ⁻	N/A	-2161.716635	0.224026	0.022416	678.306269	0.077028	-2161.470193	-2162.288971	-2162.119557
AMP-luc ⁻ to 1 TS	-328.0	-2312.082999	0.223843	0.025100	728.200896	0.082694	-2311.834056	-2312.729855	-2312.563606
1	N/A	-2161.090671	0.210111	0.022350	674.000149	0.076539	-2160.858210	-2161.661358	-2161.505436
2	N/A	-2311.524542	0.218762	0.024207	709.382537	0.080557	-2311.281573	-2312.149005	-2311.986593
2 to 3 TS	-207.1	-2311.517320	0.218076	0.023304	681.617313	0.077404	-2311.275940	-2312.143436	-2311.979460
3	N/A	-2311.521377	0.218667	0.023462	687.931194	0.078121	-2311.279248	-2312.146168	-2311.982161
3 to ox-luc ^{••} TS	-594.4	-2311.494884	0.216588	0.023505	681.309104	0.077369	-2311.254791	-2312.118799	-2311.956075
ox-luc	N/A	-1440.751027	0.148059	0.013837	480.163134	0.054527	-1440.589131	-1441.085604	-1440.978234
ox-luc ^{••}	N/A	-1440.738191	0.250577	0.014242	489.374179	0.055573	-1440.473372	-1441.071637	-1440.862390
ox-luc ^{••} *	N/A	-1440.277179	0.134361	0.013696	479.185672	0.054416	-1440.129122	-1440.604100	-1440.510459
3 to 4 TS	-118.4	-2311.496292	0.217858	0.023211	675.726119	0.076735	-2311.255223	-2312.125385	-2311.961052
4	N/A	-1629.131779	0.162671	0.016260	534.064478	0.060648	-1628.952848	-1629.547346	-1629.429063
4 to ox-luc ^{••} TS	-457.6	-1629.276161	0.160590	0.018057	583.245821	0.066233	-1629.097514	-1629.696993	-1629.581570

^aAfter adding phase change correction term to the Gibbs free energy

SUPPORTING INFORMATION

Table S4. Cartesian coordinates all species used to compute the optimized geometries used to produce the data in Tables S2 and S3

a.xyz			
O	7.742842	-1.526816	0.254083
C	6.560653	-0.865680	0.174441
C	5.347881	-1.533638	0.046778
H	5.309087	-2.618582	0.005210
C	4.192224	-0.752943	-0.024227
S	2.539557	-1.275135	-0.181695
C	4.239295	0.655322	0.028873
N	3.010457	1.282690	-0.047420
C	5.478499	1.303520	0.156493
H	5.518966	2.387441	0.198131
C	6.627752	0.543319	0.228114
H	7.601243	1.012001	0.328050
C	2.060632	0.413311	-0.155712
C	0.645510	0.781673	-0.263850
N	-0.275155	-0.087774	-0.379416
S	0.207131	2.503097	-0.264867
C	-1.541841	2.002556	-0.090980
C	-1.570516	0.537467	-0.584464
H	-2.175874	2.649339	-0.696075
H	-1.825315	2.083621	0.961645
C	-2.663431	-0.241045	0.114071
H	-1.791551	0.510658	-1.661617
O	-2.540382	-1.211053	0.804280
O	-3.875208	0.344466	-0.147195
P	-5.274633	-0.220693	0.512024
O	-5.383235	-0.115304	1.970846
O	-6.306713	0.710820	-0.260293
O	-5.421387	-1.692508	-0.040878
C	-5.340726	-1.988001	-1.451976
H	-4.399339	-1.621130	-1.869792
H	-5.378327	-3.072713	-1.533826
H	-6.192628	-1.551445	-1.979761
H	7.596372	-2.483898	0.210626
H	-6.180220	0.791302	-1.222189
c.xyz			
O	7.785052	-1.559981	0.218687
C	6.699005	-0.914329	0.164051
C	5.418158	-1.559259	0.041638
H	5.386026	-2.644005	-0.004364
C	4.265765	-0.794399	-0.014559
S	2.603982	-1.329029	-0.162921
C	4.279309	0.626142	0.043297
N	3.053800	1.231545	-0.022528
C	5.525403	1.282852	0.165340
H	5.549544	2.369193	0.212562
C	6.679592	0.542871	0.221940
H	7.642583	1.038597	0.315613
C	2.096043	0.359860	-0.128671
C	0.693799	0.723227	-0.241017
N	-0.249960	-0.131053	-0.335475
S	0.271228	2.456298	-0.294947
C	-1.482691	1.986910	-0.111990
C	-1.529178	0.510691	-0.572883
H	-2.108259	2.627829	-0.732231
H	-1.769684	2.094123	0.937788
C	-2.647634	-0.216377	0.138963
H	-1.745524	0.466348	-1.650185
O	-2.553963	-1.112469	0.927077
O	-3.852144	0.327474	-0.233877
P	-5.271367	-0.144039	0.451652
O	-5.424629	0.161431	1.878310
O	-6.278163	0.670827	-0.472715
O	-5.411032	-1.678596	0.105120
C	-5.287469	-2.165930	-1.247984
H	-4.337416	-1.850224	-1.687033
H	-5.314832	-3.251748	-1.179509
H	-6.127190	-1.815729	-1.853609
H	-6.116553	0.623398	-1.431485
d.xyz			
O	7.779380	-1.446203	-0.078294
C	6.583816	-0.792850	-0.071498
C	5.373726	-1.468812	0.063819
H	5.349928	-2.550265	0.170306
C	4.204386	-0.708021	0.057572
S	2.552688	-1.254972	0.202240
C	4.224686	0.694854	-0.078726
N	2.983853	1.310615	-0.068179
C	5.457508	1.348508	-0.212754
H	5.485586	2.428752	-0.319188
C	6.626879	0.605664	-0.209075
H	7.592939	1.089316	-0.312340
C	2.029415	0.435425	0.067613
e.xyz			
O	7.752545	-1.583505	0.228328
C	6.669257	-0.931368	0.172297
C	5.386454	-1.568001	0.033558
H	5.348948	-2.652073	-0.024324
C	4.237284	-0.796899	-0.022511
S	2.574015	-1.322517	-0.188220
C	4.256851	0.621701	0.050586
N	3.032414	1.234173	-0.017075
C	5.504391	1.270656	0.188163
H	5.533702	2.356363	0.246929
C	6.655603	0.524430	0.245198
H	7.619877	1.015372	0.350801
C	2.072674	0.368570	-0.139120
C	0.668767	0.734799	-0.254759
N	-0.273056	-0.116685	-0.366116
S	0.245211	2.469897	-0.285961
C	-1.509175	1.991916	-0.123682
C	-1.557948	0.521456	-0.597691
H	-2.131815	2.639966	-0.739319
H	-1.804507	2.087773	0.925024
C	-2.696256	-0.202896	0.108121
H	-1.761654	0.489057	-1.676985
O	-2.551980	-1.077370	0.926062
O	-3.864192	0.301092	-0.303617
P	-5.390452	-0.071310	0.380668
O	-5.351180	0.248048	1.836209
O	-6.338341	0.572889	-0.579417
O	-5.408914	-1.685727	0.208078
C	-5.381026	-2.221933	-1.111800
H	-4.422787	-2.006900	-1.599730
H	-5.497091	-3.303265	-1.020472
H	-6.195777	-1.815120	-1.718021
f.xyz			
O	7.761045	-1.515246	-0.010595
C	6.575943	-0.836067	-0.023897
C	5.348607	-1.491433	0.067938
H	5.304338	-2.574135	0.156222
C	4.192209	-0.713981	0.043126
S	2.526941	-1.243057	0.133507
C	4.233067	0.692321	-0.069246
N	3.005592	1.330624	-0.082705
C	5.481890	1.322475	-0.157844
H	5.532848	2.403877	-0.244681
C	6.642690	0.560310	-0.135752
H	7.617538	1.032829	-0.204652
C	2.020586	0.467350	0.013500
C	0.646636	0.792066	0.027564
N	-0.322168	-0.094936	0.122977
S	0.085181	2.501598	-0.079685
C	-1.662407	1.927827	-0.007574
C	-1.546059	0.413669	0.118471
H	-2.193045	2.235778	-0.913931
H	-2.168221	2.385180	0.847973
C	-2.705427	-0.444327	0.211746
O	-2.709532	-1.662704	0.316078
O	-3.848441	0.303457	0.149162
P	-5.408839	-0.267840	0.413739
O	-5.500688	-0.922635	1.753792
O	-6.265913	0.903757	0.035648
O	-5.531017	-1.433021	-0.721449
C	-5.322614	-1.062381	-2.077534
H	-4.272789	-0.796470	-2.252045

SUPPORTING INFORMATION

H	-5.574703	-1.928172	-2.693531	C	-0.083845	-3.449668	0.933325
H	-5.960621	-0.218044	-2.359273	C	0.017480	-0.723892	0.168667
H	7.594958	-2.465547	0.070701	H	2.196254	-0.169622	-1.400435
g.xyz				H	3.976996	-1.728716	-2.026865
O	7.789825	-1.571719	0.026527	C	-1.070870	-1.253615	0.838951
C	6.704206	-0.902080	-0.001677	C	-1.122875	-2.611330	1.237020
C	5.410682	-1.520708	0.088042	H	-1.995173	-2.956571	1.782997
H	5.360444	-2.602556	0.182973	C	-1.122993	2.611280	-1.237017
C	4.258513	-0.744677	0.053724	C	-0.084001	3.449665	-0.933321
S	2.583909	-1.274358	0.142993	C	1.029323	2.978203	-0.184368
C	4.282078	0.662386	-0.069515	C	1.075176	1.612431	0.223521
N	3.043327	1.289829	-0.093489	C	0.017448	0.723892	-0.168668
C	5.534599	1.292773	-0.159715	C	-1.070926	1.253567	-0.838951
H	5.578265	2.376032	-0.256061	H	2.034113	4.891529	-0.145405
C	6.695470	0.539971	-0.127791	H	-1.995308	2.956483	-1.782992
H	7.662388	1.033311	-0.198712	H	-0.105939	4.491598	-1.241451
C	2.069396	0.429789	0.006222	C	2.083812	3.857312	0.186014
C	0.677471	0.755127	0.010797	C	2.163074	1.193491	1.041717
N	-0.286470	-0.112511	0.123331	C	3.160983	2.069819	1.396387
S	0.137827	2.471874	-0.117933	C	3.132413	3.415848	0.954540
C	-1.618073	1.917446	-0.102284	H	2.196249	0.169717	1.400429
C	-1.526764	0.408691	0.103211	H	3.976922	1.728890	2.026860
H	-2.097952	2.191958	-1.048220	H	3.931393	4.094706	1.236484
H	-2.154201	2.429607	0.702016	O	-2.118531	-0.440866	1.183981
C	-2.677906	-0.427597	0.201963	O	-2.118550	0.440771	-1.183981
O	-2.713586	-1.646482	0.361948	P	-3.210022	-0.000071	-0.000000
O	-3.826859	0.325494	0.062471	O	-3.915439	1.201184	0.534366
P	-5.381962	-0.183085	0.401587	O	-3.915389	-1.201354	-0.534366
O	-5.488518	-0.660404	1.816036	CO2.xyz			
O	-6.232931	0.940770	-0.117955	O	0.000000	-0.000000	1.162759
O	-5.543865	-1.486689	-0.570651	C	0.000000	0.000000	0.000000
C	-5.267285	-1.316186	-1.952292	O	0.000000	-0.000000	-1.162759
H	-4.196108	-1.146577	-2.116006	5xyz			
H	-5.561185	-2.237290	-2.460800	C	-1.820464	0.083596	-0.067256
H	-5.834829	-0.477077	-2.369975	O	-2.835202	-0.427842	-0.574858
Href.xyz				O	-0.613867	-0.348635	-0.692897
-1.630201	4.320959	-0.965516	C	0.827581	-0.573398	0.062799	
C	-0.502523	4.340127	-0.183728	O	0.670095	-1.427282	1.289153
C	0.141381	3.129832	0.194013	O	1.772356	-0.977062	-1.040668
C	-0.410810	1.882122	-0.220211	O	1.244480	0.926311	0.587047
C	-1.565422	1.897342	-1.052132	C	1.152446	1.987779	-0.345850
C	-2.155860	3.084065	-1.414224	H	0.102754	2.202076	-0.576680
H	1.748980	4.112441	1.264443	H	1.605853	2.870866	0.112683
H	-2.114034	5.249079	-1.253630	H	1.691849	1.753543	-1.272123
H	-0.073324	5.280270	0.152438	O	-1.713620	0.922790	0.841319
C	1.342607	3.154203	0.953543	H2O2.xyz			
C	0.232947	0.662064	0.180133	O	0.703698	0.109897	-0.063895
H	-1.975349	0.960915	-1.416159	O	-0.703877	-0.110093	-0.063568
H	-3.031827	3.074639	-2.055786	H	-1.017402	0.609069	0.509351
C	1.427511	0.762811	0.861499	H	1.018832	-0.607500	0.510356
C	1.993034	1.990157	1.266685	HOO-.xyz			
H	2.924815	1.982467	1.823150	O	0.055511	0.790000	-0.000000
C	0.035148	-2.864724	-1.225346	O	0.055511	-0.680438	0.000000
C	-1.247480	-3.241392	-0.927838	H	-0.888183	-0.876497	0.000000
C	-2.101148	-2.380699	-0.184997	6.xyz			
C	-1.631086	-1.099811	0.228822	P	-0.478739	0.207147	0.000000
C	-0.312295	-0.679818	-0.155391	O	-0.836952	-0.551152	1.288633
C	0.480785	-1.590076	-0.819963	O	-0.836952	1.696545	0.000000
H	-3.756901	-3.770127	-0.157455	O	-0.836952	-0.551152	-1.288633
H	0.716534	-3.513970	-1.765309	O	1.232398	0.257960	0.000000
H	-1.621137	-4.213387	-1.237131	C	1.872123	-0.989371	0.000000
C	-3.412476	-2.794947	0.176723	H	1.609411	-1.580145	0.890322
C	-2.480618	-0.298362	1.041933	H	1.609411	-1.580145	-0.890322
C	-3.737670	-0.732527	1.387585	H	2.957181	-0.828296	0.000000
C	-4.218093	-1.988246	0.940729	O2--.xyz			
H	-2.125536	0.660894	1.404158	O	0.000000	0.000000	0.661719
H	-4.367960	-0.109132	2.014576	O	0.000000	-0.000000	-0.661719
H	-5.216585	-2.312990	1.216505	3 to 4TS.xyz			
O	2.124448	-0.396542	1.204761	O	-8.190274	-0.949107	-0.049395
O	1.790388	-1.237261	-1.151270	C	-6.934744	-0.434992	-0.038249
P	2.881116	-1.210133	0.037474	C	-5.803979	-1.243838	-0.050563
O	3.405006	-2.492705	0.520722	H	-5.890525	-2.326914	-0.070077
O	3.995717	-0.262168	-0.577762	C	-4.561502	-0.605580	-0.035532
H	3.664729	0.541841	-1.017424	S	-2.975353	-1.320214	-0.042212
ref.xyz				C	-4.445588	0.799874	-0.008301
C	3.132565	-3.415710	-0.954541	N	-3.150060	1.277374	0.004885
C	2.083985	-3.857219	-0.186012	C	-5.605494	1.592071	0.002038
C	1.029457	-2.978157	0.184370	H	-5.519551	2.673948	0.021728
C	1.075248	-1.612383	-0.223522	C	-6.838284	0.973486	-0.012789
C	2.163126	-1.193396	-1.041720	H	-7.754568	1.554510	-0.004928
C	3.161073	-2.069681	-1.396391				
H	-0.105735	-4.491601	1.241457				
H	3.931575	-4.094532	-1.236484				
H	2.034333	-4.891437	0.145409				

SUPPORTING INFORMATION

C	-5.336305	-1.500392	-0.059095	N	-1.148450	-0.274301	0.000000
H	-5.295385	-2.582764	-0.145400	C	-1.877083	-2.635000	0.000000
C	-4.178873	-0.721214	-0.039409	H	-2.925653	-2.349767	0.000000
S	-2.521198	-1.245403	-0.132964	C	-1.496883	-3.947746	0.000000
C	-4.225606	0.686001	0.070238	H	-2.236419	-4.743501	0.000000
N	-3.000478	1.316269	0.077983	C	0.000000	0.429475	0.000000
C	-5.472292	1.327820	0.162713	C	0.065877	1.837769	0.000000
H	-5.515975	2.409169	0.247190	N	1.211813	2.519219	0.000000
C	-6.624523	0.567582	0.145990	S	-1.439487	2.773514	0.000000
H	-7.601508	1.034440	0.216877	C	-0.457713	4.296832	0.000000
C	-2.033610	0.447609	-0.019356	C	1.020118	3.869615	0.000000
C	-0.646881	0.803674	-0.035036	H	-0.669108	4.896970	0.888891
N	0.320293	-0.111206	-0.129528	H	-0.669108	4.896970	0.888891
S	-0.124591	2.471658	0.070541	O	1.914512	4.714411	0.000000
C	1.612854	1.919481	-0.016051				
C	1.519591	0.423200	-0.123979	AMP-luc- to 1 TS.xyz			
H	2.154617	2.233785	0.881902	O	-7.894154	-1.258433	-0.483944
H	2.108349	2.362617	-0.885996	C	-6.673114	-0.662431	-0.411793
C	2.725927	-0.438059	-0.223942	C	-5.496861	-1.397975	-0.302846
O	2.682207	-1.643171	-0.333254	H	-5.518217	-2.484144	-0.272033
O	3.831440	0.311283	-0.164662	C	-4.297144	-0.687172	-0.235826
P	5.424494	-0.275983	-0.412209	S	-2.674503	-1.308172	-0.094219
O	5.478738	-0.946328	-1.741613	C	-4.259829	0.721057	-0.277181
O	6.259642	0.908150	-0.047097	N	-2.993799	1.278769	-0.206462
O	5.502419	-1.413187	0.742830	C	-5.460964	1.436673	-0.387236
C	5.412675	-0.999065	2.103871	H	-5.441321	2.521745	-0.419889
H	4.417950	-0.592776	2.322685	C	-6.657220	0.745018	-0.453534
H	5.576671	-1.885464	2.718981	H	-7.601580	1.272692	-0.539400
H	6.170990	-0.245561	2.335352	C	-2.087481	0.356068	-0.112026
H	-7.589424	-2.454747	-0.049689	C	-0.665606	0.618827	-0.023964
				N	0.217248	-0.315676	0.056973
ox-luc.xyz				S	-0.060815	2.298191	-0.037691
O	0.237113	-5.551744	0.000000	C	1.655521	1.650020	-0.100021
C	-0.057633	-4.229098	0.000000	C	1.495118	0.167847	0.239562
C	0.930597	-3.252117	0.000000	H	2.272285	2.190322	0.620427
H	1.982836	-3.520599	0.000000	H	2.069613	1.808715	-1.102535
C	0.510914	-1.920020	0.000000	C	2.617236	-0.747466	0.043145
S	1.482573	-0.479360	0.000000	H	1.363572	0.205026	1.782966
C	-0.857187	-1.568678	0.000000	O	2.550501	-1.962300	-0.033052
N	-1.108202	-0.215708	0.000000	O	3.783755	-0.061735	0.010841
C	-1.834789	-2.580051	0.000000	P	5.278053	-0.798675	-0.306808
H	-2.886717	-2.312852	0.000000	O	5.705274	-1.596471	0.881287
C	-1.432007	-3.897447	0.000000	O	5.238716	-1.341058	-1.702091
H	-2.157997	-4.703773	0.000000	O	6.129620	0.595043	-0.273083
C	0.000000	0.454237	0.000000	C	5.913394	1.533992	-1.320884
C	0.042180	1.913787	0.000000	H	6.595014	2.369968	-1.150402
N	1.158447	2.559242	0.000000	H	6.122142	1.086413	-2.297312
S	-1.476011	2.794229	0.000000	H	4.881768	1.904307	-1.305194
C	-0.532990	4.339277	0.000000	O	1.077102	0.282033	2.835751
C	0.944822	3.950089	0.000000	O	-0.267609	0.135177	2.882611
H	-0.758068	4.929739	0.891181	H	-7.797084	-2.221678	-0.448446
H	-0.758068	4.929739	-0.891181				
O	1.842924	4.759093	0.000000	AMP-luc-xyz			
H	1.197556	-5.683558	0.000000	O	7.717587	-1.544258	0.237811
				C	6.536492	-0.879015	0.169256
Ox-luc*.xyz				C	5.322073	-1.542320	0.033192
O	0.271430	-5.508280	0.000000	H	5.280966	-2.626502	-0.023739
C	-0.051566	-4.225043	0.000000	C	4.167890	-0.758394	-0.027036
C	0.951893	-3.212899	0.000000	S	2.513947	-1.274331	-0.194056
H	2.001829	-3.491862	0.000000	C	4.218108	0.648652	0.044847
C	0.532565	-1.911193	0.000000	N	2.990437	1.280395	-0.026519
S	1.503847	-0.450616	0.000000	C	5.458442	1.292123	0.181895
C	-0.869759	-1.558985	0.000000	H	5.501202	2.375306	0.238437
N	-1.149710	-0.258887	0.000000	C	6.606535	0.528605	0.242956
C	-1.849539	-2.612513	0.000000	H	7.581002	0.993957	0.349079
H	-2.901534	-2.346633	0.000000	C	2.038382	0.415528	-0.148126
C	-1.440633	-3.915458	0.000000	C	0.623427	0.785836	-0.262658
H	-2.149913	-4.736382	0.000000	N	-0.297503	-0.080261	-0.388443
C	0.000000	0.471485	0.000000	S	0.187879	2.510026	-0.265726
C	0.031834	1.872757	0.000000	C	-1.564031	2.008842	-0.121507
N	1.167653	2.570885	0.000000	C	-1.594200	0.541790	-0.607846
S	-1.492890	2.775342	0.000000	H	-2.187427	2.655403	-0.737639
C	-0.539398	4.315535	0.000000	H	-1.866446	2.095442	0.925698
C	0.947106	3.919037	0.000000	C	-2.717199	-0.212983	0.091542
H	-0.764082	4.910292	0.889173	H	-1.794273	0.512817	-1.687758
H	-0.764082	4.910292	-0.889173	O	-2.553087	-1.115437	0.874442
O	1.824102	4.777856	0.000000	O	-3.891523	0.298574	-0.285300
H	1.237595	-5.638259	0.000000	P	-5.407234	-0.108605	0.407479
				O	-5.342633	0.153570	1.873039
Ox-luc--.xyz				O	-6.370891	0.569203	-0.512308
O	0.253075	-5.552797	0.000000	O	-5.418980	-1.714343	0.171215
C	-0.092863	-4.352362	0.000000	C	-5.417942	-2.197879	-1.169508
C	0.905287	-3.281591	0.000000	H	-4.472967	-1.955530	-1.670359
H	1.953957	-3.563587	0.000000	H	-5.523717	-3.282840	-1.118230
C	0.492261	-1.974801	0.000000	H	-6.249608	-1.774097	-1.739900
S	1.486083	-0.522893	0.000000	H	7.568377	-2.500116	0.180249
C	-0.889573	-1.601247	0.000000				

SUPPORTING INFORMATION

2 to 3 TS.xyz

O	-7.831332	-1.208142	-0.655364
C	-6.611779	-0.628101	-0.509770
C	-5.475967	-1.364929	-0.193433
H	-5.528098	-2.440746	-0.050803
C	-4.273045	-0.666191	-0.067081
S	-2.693518	-1.287466	0.318044
C	-4.198538	0.729171	-0.251492
N	-2.935563	1.271866	-0.094236
C	-5.361296	1.448176	-0.570227
H	-5.309265	2.523033	-0.713189
C	-6.556991	0.769209	-0.697100
H	-7.473749	1.295407	-0.942483
C	-2.075946	0.352937	0.198112
C	-0.648892	0.612806	0.435850
N	0.164780	-0.317321	0.725120
S	-0.068345	2.287684	0.339407
C	1.623011	1.665170	0.609919
C	1.511466	0.181606	1.029783
H	2.111307	2.239396	1.398028
H	2.194303	1.754688	-0.318565
C	2.587565	-0.729860	0.381378
O	1.794117	-0.006838	2.371657
O	2.360641	-1.600251	-0.437547
O	3.832442	-0.128211	0.481611
P	4.721239	0.353250	-0.839371
O	3.850645	1.144301	-1.772260
O	5.975749	0.930633	-0.249613
O	5.061904	-1.056625	-1.590685
C	5.669999	-2.081739	-0.819392
H	4.974466	-2.451162	-0.057535
H	5.921105	-2.897394	-1.501486
H	6.585812	-1.722723	-0.335986
O	2.445833	-1.306096	2.278382
H	-7.766684	-2.164258	-0.511542

2.xyz

O	-7.704595	-1.703433	-0.085711
C	-6.529583	-1.028256	-0.178548
C	-5.343498	-1.533771	0.341744
H	-5.319286	-2.495204	0.846691
C	-4.192750	-0.757312	0.187084
S	-2.570211	-1.104901	0.713188
C	-4.218920	0.491218	-0.466140
N	-2.997213	1.136696	-0.540208
C	-5.430802	0.978556	-0.979977
H	-5.455762	1.939989	-1.483373
C	-6.575286	0.219631	-0.834819
H	-7.527830	0.567298	-1.221038
C	-2.072210	0.432498	0.022428
C	-0.664536	0.849189	0.105539
N	0.218427	0.122309	0.647260
S	-0.210912	2.417505	-0.592764
C	1.502575	2.127688	-0.062108
C	1.550100	0.742809	0.667487
H	1.788539	2.880076	0.672375
H	2.155060	2.157431	-0.936610
C	2.512110	-0.180979	-0.109701
O	2.024988	0.858297	1.952755
O	2.137430	-1.086748	-0.815537
O	3.777798	0.195836	0.061564
P	5.110099	-0.470760	-0.775368
O	4.886005	-0.315207	-2.241520
O	6.278817	0.125909	-0.057678
O	4.948147	-2.042138	-0.394100
C	5.063075	-2.415341	0.976163
H	4.240665	-1.993101	1.566031
H	5.006314	-3.504620	1.017299
H	6.017139	-2.081454	1.394757
O	1.196905	1.813009	2.668276
H	-7.572469	-2.543477	0.378938

SUPPORTING INFORMATION

Author Contributions

S.C., M.L.C, M.G, M.B. and M.M.T.E-T conceived the study. M.B performed most of the experiments and experimental data analysis. M.L.C., L.J.Y. and I.C.R. determined the electrochemiluminescence reaction mechanism. M.M.T.E-T and M.G. developed the spectral tuning theoretical model. N.D., M.L.C., M.G., and S.C. supervised the project. S.C., M.G., M.M.T.E-T, M.B., and M.L.C. wrote the manuscript with contributions from all authors.

References

- [1] E. H. White, E. Rapaport, H. H. Seliger, T. A. Hopkins, *Bioorg. Chem.* **1971**, *1*, 92–122.
- [2] E. H. White, M. G. Steinmetz, J. D. Miano, P. D. Wildes, R. Morland, *J. Am. Chem. Soc.* **1980**, *102*, 3199–3208.
- [3] J. Miller, J. C. Miller, *Statistics and chemometrics for analytical chemistry*, Pearson education, **2018**.
- [4] J. Schindelin, I. Arganda-Carreras, E. Frise, V. Kaynig, M. Longair, T. Pietzsch, S. Preibisch, C. Rueden, S. Saalfeld, B. Schmid, J.-Y. Tinevez, D. J. White, V. Hartenstein, K. Eliceiri, P. Tomancak, A. Cardona, *Nat. Methods* **2012**, *9*, 676–682.
- [5] a) H. C. Berg, in *Random Walks in Biology*, Princeton University Press, **2018**; b) R. G. Compton, C. E. Banks, *Understanding voltammetry*, World Scientific, **2018**.
- [6] N. Suzuki, M. Sato, K. Okada, T. Goto, *Tetrahedron* **1972**, *28*, 4065–4074.
- [7] T. Ohsaka, Y. Shintani, F. Matsumoto, T. Okajima, K. Tokuda, *Bioelectrochem. Bioenerg.* **1995**, *37*, 73–76.
- [8] M. J. Frisch, G. W. Trucks, H. B. Schlegel, G. E. Scuseria, M. A. Robb, J. R. Cheeseman, G. Scalmani, V. Barone, G. A. Petersson, H. Nakatsuji, X. Li, M. Caricato, A. V. Marenich, J. Bloino, B. G. Janesko, R. Gomperts, B. Mennucci, H. P. Hratchian, J. V. Ortiz, A. F. Izmaylov, J. L. Sonnenberg, Williams, F. Ding, F. Lipparini, F. Egidi, J. Goings, B. Peng, A. Petrone, T. Henderson, D. Ranasinghe, V. G. Zakrzewski, J. Gao, N. Rega, G. Zheng, W. Liang, M. Hada, M. Ehara, K. Toyota, R. Fukuda, J. Hasegawa, M. Ishida, T. Nakajima, Y. Honda, O. Kitao, H. Nakai, T. Vreven, K. Throssell, J. A. Montgomery Jr., J. E. Peralta, F. Ogliaro, M. J. Bearpark, J. J. Heyd, E. N. Brothers, K. N. Kudin, V. N. Staroverov, T. A. Keith, R. Kobayashi, J. Normand, K. Raghavachari, A. P. Rendell, J. C. Burant, S. S. Iyengar, J. Tomasi, M. Cossi, J. M. Millam, M. Klene, C. Adamo, R. Cammi, J. W. Ochterski, R. L. Martin, K. Morokuma, O. Farkas, J. B. Foresman, D. J. Fox, Wallingford, CT, **2016**.
- [9] A. V. Marenich, C. J. Cramer, D. G. Truhlar, *J. Phys. Chem. B* **2009**, *113*, 6378–6396.
- [10] E. I. Izgorodina, C. Y. Lin, M. L. Coote, *Phys. Chem. Chem. Phys.* **2007**, *9*, 2507–2516.
- [11] F. Weigend, R. Ahlrichs, *Phys. Chem. Chem. Phys.* **2005**, *7*, 3297–3305.
- [12] R. F. Ribeiro, A. V. Marenich, C. J. Cramer, D. G. Truhlar, *J. Phys. Chem. B* **2011**, *115*, 14556–14562.
- [13] V. Lockett, M. Horne, R. Sedev, T. Rodopoulos, J. Ralston, *Phys. Chem. Chem. Phys.* **2010**, *12*, 12499–12512.
- [14] P. Christ, A. G. Lindsay, S. S. Vormittag, J. M. Neudörfl, A. Berkessel, A. C. O'Donoghue, *Chem. – Eur. J.* **2011**, *17*, 8524–8528.
- [15] a) D. Case, I. Ben-Shalom, S. Brozell, D. Cerutti, T. Cheatham III, V. Cruzeiro, T. Darden, R. Duke, D. Ghoreishi, M. Gilson, *University of California, San Francisco* **2018**; b) N. Homeyer, A. H. Horn, H. Lanig, H. Sticht, *J. Mol. Model.* **2006**, *12*, 281–289.
- [16] a) L. Hedin, B. I. Lundqvist, *J. Phys. C: Solid State Phys.* **1971**, *4*, 2064; b) C. Lee, W. Yang, R. G. Parr, *Phys. Rev. B* **1988**, *37*, 785–789; c) E. Cancas, B. Mennucci, J. Tomasi, *J. Chem. Phys.* **1997**, *107*, 3032–3041.
- [17] R. Krishnan, J. S. Binkley, R. Seeger, J. A. Pople, *J. Chem. Phys.* **1980**, *72*, 650–654.
- [18] J. Wang, W. Wang, P. A. Kollman, D. A. Case, *J. Mol. Graphics Modell.* **2006**, *25*, 247–260.
- [19] T. Fox, P. A. Kollman, *J. Phys. Chem. B* **1998**, *102*, 8070–8079.
- [20] F.-Y. Dupradeau, A. Pigache, T. Zaffran, C. Savineau, R. Lelong, N. Grivel, D. Lelong, W. Rosanski, P. Cieplak, *Phys. Chem. Chem. Phys.* **2010**, *12*, 7821–7839.
- [21] H. J. Berendsen, J. v. Postma, W. F. Van Gunsteren, A. DiNola, J. R. Haak, *J. Chem. Phys.* **1984**, *81*, 3684–3690.
- [22] P. Altoè, M. Stenta, A. Bottoni, M. Garavelli, in *AIP Conference Proceedings*, Vol. 963, American Institute of Physics, **2007**, pp. 491–505.
- [23] F. Aquilante, J. Autschbach, R. K. Carlson, L. F. Chibotaru, M. G. Delcey, L. De Vico, I. Fdez. Galván, N. Ferré, L. M. Frutos, L. Gagliardi, M. Garavelli, A. Giussani, C. E. Hoyer, G. Li Manni, H. Lischka, D. Ma, P. Å. Malmqvist, T. Müller, A. Nenov, M. Olivucci, T. B. Pedersen, D. Peng, F. Plasser, B. Pritchard, M. Reiher, I. Rivalta, I. Schapiro, J. Segarra-Martí, M. Stenrup, D. G. Truhlar, L. Ungur, A. Valentini, S. Vancocillie, V. Veryazov, V. P. Vysotskiy, O. Weingart, F. Zapata, R. Lindh, *J. Comput. Chem.* **2016**, *37*, 506–541.
- [24] B. O. Roos, P. R. Taylor, P. E. M. Sigbahn, *Chem. Phys.* **1980**, *48*, 157–173.
- [25] K. Pierloot, B. Dumez, P.-O. Widmark, B. O. Roos, *Theor. Chim. Acc.* **1995**, *90*, 87–114.
- [26] a) M. M. El-Tahawy, A. Nenov, M. Garavelli, *J. Chem. Theory Comput.* **2016**, *12*, 4460–4475; b) A. Bonvicini, B. Demoulin, S. F. Altavilla, A. Nenov, M. M. El-Tahawy, J. Segarra-Martí, A. Giussani, V. S. Batista, M. Garavelli, I. Rivalta, *Theor. Chem. Acc.* **2016**, *135*, 1–10; c) M. M. El-Tahawy, A. Nenov, O. Weingart, M. Olivucci, M. Garavelli, *J. Phys. Chem. Lett.* **2018**, *9*, 3315–3322.
- [27] G. Ghigo, B. O. Roos, P.-Å. Malmqvist, *Chem. Phys. Lett.* **2004**, *396*, 142–149.
- [28] N. Forsberg, P.-Å. Malmqvist, *Chem. Phys. Lett.* **1997**, *274*, 196–204.
- [29] T. Shiozaki, W. Györfy, P. Celani, H.-J. Werner, *J. Chem. Phys.* **2011**, *135*, 081106.
- [30] E. Johnson, K. H. Pool, R. Hamm, *Anal. Chem.* **1966**, *38*, 183–185.